



CARE/JRA1 SRF Annual Report 2007

Research and Development on Superconducting Radio-Frequency Technology for Accelerator Applications

Participating Laboratories and Institutes:

Institute (Participating number)	Acronym	Country	Coordinator	SRF Scientific Contact	Associated to
DESY (6)	DESY	D	D. Proch	D. Proch	
CEA/DSM/DAPNIA (1)	CEA	F	O. Napoly	O. Napoly	
CNRS-IN2P3-Orsay (3)	CNRS-Orsay	F	T.Garvey	T.Garvey	CNRS
INFN Legnaro (10)	INFN-LNL	I	S. Guiducci	E. Palmieri	INFN
INFN Milano (10)	INFN-Mi	I	S. Guiducci	P. Michelato	INFN
INFN Roma2 (10)	INFN-Ro2	I	S. Guiducci	S. Tazzari	INFN
INFN Frascati (10)	INFN-LNF	I	S. Guiducci	M. Castellano	INFN
Paul Scherrer Institute (19)	PSI	CH	V. Schlott	V. Schlott	
Technical University of Lodz (12)	TUL	PL	A.Napieralski	M. Grecki	
Warsaw University of Technology (14)	WUT-ISE	PL	R.Romaniuk	R. Romaniuk	
IPJ Swierk (13)	IPJ	PL	M. Sadowski	M. Sadowski	

Industrial Involvement:

Company Name	Country	Contact Person
ACCEL Instruments GmbH	D	M. Peiniger
WSK Mess- und Datentechnik GmbH	D	F. Schölz
E. ZANON SPA	I	G. Corniani
Henkel Lohnpoliertechnik GmbH	D	B. Henkel

Acknowledgment

Work supported by the European Community-Research Infrastructure Activity under the FP6 “Structuring the European Research Area” programme (CARE, contract number RII3-CT 2003-506395).

Table of contents

1. Executive Summary	3
2. List of Work packages, tasks and responsibilities	5
3. Status of Deliverables	6
4. List of major meetings organized under JRA1	8
5. List of talks from JRA1 members	9
6. List of publications	10
7. Report of the International Advisory Committee	17
8. Status of Activities	19
WP2 Improved standard cavity fabrication	19
WP3 Seamless cavity production	23
WP4 Thin film cavity production	28
WP5 Surface preparation	34
WP6 Material analysis	38
WP7 Couplers	44
WP8 Tuners	48
WP9 Low level RF	54
WP10 Cryostat integration test	63
WP11 Beam diagnostics	65

1. Executive Summary

The aim of the JRA on Superconducting RF Technology is to improve the quality and performance of the superconducting test accelerator TTF (Tesla Test Facility), a unique test facility to explore the operating conditions of a high gradient superconducting accelerator, at DESY.

The ultimate objectives of this research activity are

- to increase the accelerating gradient from 25 to 35 MV/m and
- to increase the quality factor from 5×10^9 to 2×10^{10} ,
- to improve the reliability, operating performance and availability of the superconducting accelerating system,
- to achieve a cost reduction of the SRF cavities and their associated components.

Great progress has been made by the group of W. Singer (WP3.2) in fabrication of the first 9-cell hydroformed cavity and also a 9-cell cavity from large grain material. Based on these results it can be expected to fabricate high gradient and high Q (low RF loss) cavities at reduced material and processing costs. Excellent results on electro polishing followed by alcohol rinsing have been reported in a highlight talk at the CARE07 annual meeting at CERN. The progress of this work follows the experience of intensive EP studies of Niobium cavities at the labs and also by industrial studies. A further highlight in 2007 was the very successful test of the beam position monitor of WP11. This BPM will be used in FLASH and also in the XFEL accelerator.

Some tasks which are due at the end of 2007 will continue in 2008. Among these tasks are those with high risk, such as dry ice cleaning and thin film.

Use and Dissemination of knowledge.

Communication is an important aspect of the JRA-SRF, both between participating institutes as well as with external institutes who share our interest in high gradient, low loss superconducting cavities. Contributions from JRA-SRF members were given to several conferences and meetings, the major ones being as follows:

- The XXth IEEE-SPIE WILGA Joint Symposium on Photonics, Web Engineering, Electronics for High Energy Physics Experiments, (Wilga, PL)
- The IEEE-EUROCON 2007, Int. Conference on Computer as a Tool, (Warsaw, PL)
- The Particle Accelerator Conference 2007 (Albuquerque, USA)
- The MIXDES 2007, Int. Conference on Mixed Design of Integrated Circuits and Systems (Ciechocinek, PL)
- The Asia Particle Accelerator Conference 2007 (Indore, India)
- The TESLA Technology Collaboration Meeting (FNAL-Chicago, USA)
- The Int. Workshop on SRF 2007 (Beijing, China)
- Several GDE/ILC meetings

Papers and talks were also presented at TESLA Technology Collaboration meetings in this reporting year as well as at the annual CARE meeting held at CERN in November

The impressive progress made in WP5 (Electro Polishing) and WP10 (Beam Position Monitors) has been presented as highlight talks at the CARE 07 annual meeting. The presentations can be found on the meeting WEB site.

Annual SRF Meeting















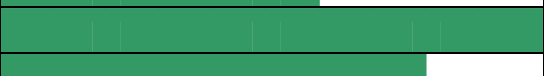

In addition to the above conferences and several telephone meetings, the SRF JRA community held their dedicated annual meeting in Warsaw, September 17-19, 2007 and during the annual CARE07 meeting at CERN, October 29-31, 2007. The meeting in Warsaw included an entire review of all work-packages and tasks therein. It was the opportunity for the external scientific advisory committee to review the program of work. Their findings can be found later within this report. What was clear from the Warsaw meeting is that, despite some delay in certain milestones / deliverables, the project has made enormous progress in the last twelve months. The technical summaries to be found in later sections bears witness to this.

The strong connection between the R&D activities in JRA-SRF, the European X-FEL, and the TTC (TESLA technology Collaboration) community continues. It is obvious that many of the results of the work from SRF will have a major impact on these project and collaboration.

2. List of Work packages, tasks and responsibilities

2	Improved Standard Cavity Fabrication (ISCF)	P. Michelato	INFN Mi
	2.1 Reliability analysis	L. Lilje	DESY
	2.2 Improved component design	P. Michelato	INFN Mi
	2.3 EB welding	J. Tiessen	DESY
3	Seamless Cavity Production (SCP)	W.-D. Moeller	DESY
	3.1 Seamless cavity production by spinning	E. Palmieri	INFN LNL
	3.2 Seamless cavity production by hydroforming	W. Singer	DESY
4	Thin Film Cavity Production (TFCP)	M. Sadowski	IPJ
	4.1 Linear arc cathode	P. Strzyzewski	IPJ
	4.2 Planar arc cathode	S. Tazzari	INFN Ro2
5	Surface Preparation (SP)	A. Matheisen	DESY
	5.1 EP on single cells	C. Antoine	CEA
	5.2 EP on multicells	N. Steinhau-Kühl	DESY
	5.3 Automated EP	E. Palmieri	INFN LNL
	5.4 Dry ice cleaning	D. Reschke	DESY
6	Material Analysis (MA)	E. Palmieri	INFN LNL
	6.1 Squid scanning	W. Singer	DESY
	6.2 Flux gate magnetometry	M. Valentino	INFN LNL
	6.3 DC field emission studies of Nb samples	X. Singer	DESY
7	Couplers (COUP)	A. Variola	CNRS-Orsay
	7.1 New proto-types	A. Variola	CNRS-Orsay
	7.2 Titanium-nitride coating system	A. Variola	CNRS-Orsay
	7.3 Conditioning studies	P. Lepercq	CNRS-Orsay
8	Tuners (TUN)	P. Sekalski	TUL
	8.1 UMI Tuner	A. Bosotti	INFN-Milano
	8.2 Magnetostrictive Tuner	A. Grecki	TUL
	8.3 CEA Tuner	P. Bosland	CEA
	8.4 IN2P3 activities	M. Fouaidy	CNRS-Orsay
9	Low Level RF (LLRF)	S. Simrock	DESY
	9.1 Operability and Technical performance	S. Simrock	DESY
	9.2 Cost and reliability	M. Grecki	TUL
	9.3 Hardware technology	R. Romaniuk	WUT-ISE
	9.4 Software technology	T. Jezynski	WUT-ISE
10	Cryostat Integration Tests	B. Visentin	CEA
11	Beam Diagnostics (BD)	M. Castellano	INFN-LNF
	11.1 Beam position monitor	C. Simon	CEA
	11.2 Emittance monitor	M. Castellano	INFN-LNF

3.) Status of Deliverables

N°	Deliverable Name	Type	Task	Lab	Planned	
2006/7	1-cell spinning parameters defined	Report	3	INFN-Leg	36	
2007 SRF						10 20 30 40 50 60 70 80 90 100
						Progress in %
5	Fabrication of new cavity with improved components	Prototype	2.2.5.2	INFN	47	
6	Fabrication Multi-cell cavities by spinning	Prototype	3.1.7.2	INFN-Leg	48	
7	Fabrication of hydroformed 9-cell cavities	Prototype	3.2.6.3	DESY	47	
8	First multicell coating with linear-arc cathode	Prototype	4.1.2.2	IPJ	48	
9	First multicell coating with planar-arc cathode	Prototype	4.2.2.4	INFN-Ro2	41	
10	Report on quality of HTc superconducting properties	Report	4.2.3.2	INFN-Ro2	48	
11	EP on single cells: parameters fixed	Report	5.1.5.2	CEA	48	
12	Evaluate oxipolishing experiments	Report	5.2.3.9	DESY	40	
13	Final report on industrial electropolishing	Report	5.2.4.8	DESY	48	
14	Automated EP: Conclude on best electrolyte	Report	5.3.5.5	INFN-Leg	44	
15	VT CO ₂ of 9-cell cavities: evaluation of experimental results	Report	5.4.4.2	DESY	48	
16	Dry ice cleaning of horizontal 9-cell cavities: evaluation of experimental results	Report	5.4.6.2	DESY	48	
17	Final report on SQUID scanning	Report	6.1.5.4	DESY	48	
18	Conclude on comparison of SQUID scanner vs. flux gate detector	Report	6.2.6.2	INFN-Leg	48	
19	DC field emission: evaluation of scanning results	Report	6.3.1.9	DESY	48	

20	DC field emission: evaluate strong emitter investigations	Report	6.3.2.6	DESY	48	
21	Prototype couplers: final report on conditioning	Report	7.3.3	CNRS-Ors	47	
22	Evaluation of INFN tuner operation	Report	8.1.10	INFN-Mi	48	
23	Cryostat integration tests: final evaluation	Report	10.6.3	CEA	46	
24	Evaluation of BPM operation	Report	11.1.12	CEA	48	
25	Evaluation of beam emittance monitor operation	Report	11.2.13	INFN-Ro	48	
26	EB Welding of prototypes of components	Prototype	2.3.3.6	DESY	48	

4. List of major meetings organized under JRA1

Date	Title/Subject	Location	Number of attendees	Website address
April 2007	WP5 Meeting onelectro polishing	Legnaro	10	
April 23-24, 2007	CARE-JRA1-WP4 Working Meeting	Tor Vergata -INFR – Rome, Italy,	9	Not available
May 23-24, 2007	CARE-JRA1-WP4 (Thin film production) Working Meeting No. 2-2007; Draft of the Midterm 2007 Report on WP4, proposals of new papers and joint experiments.	IPJ Swierk, Poland	5	None
June 7, 2007	Status of the experiment and future work of WP11	DESY	6	
June 21-23, 2007	14th International Conference Mixed Design of Integrated Circuits and Systems, special CARE session	Ciechocinek, Poland	170	www.mixdes.org
Sept. 17-19, 2007	CARE-SRF Annual Meeting 2007	Warsaw	18	https://indico.desy.de/conferenceDisplay.py?confId=438
Oct. 10-19, 2007	13th Int. Workshop on RF Superconductivity (SRF2007)	Beijing	273	http://www.pku.edu.cn/academic/srf2007/home.html
Oct. 29-31, 2007	CARE07 Annual Meeting	CERN	105	http://indico.cern.ch/conferenceDisplay.py?confId=15901

5. List of talks from JRA1 members

Date	Speaker/Lab	Event	Subject
Jan, 25, 2007	M.J. Sadowski, IPJ, Swierk, Poland	16th Symp. on Application of Plasma Proc., Podbanske, Slovakia; http://www.fmph.uniba.sk/sa	Deposition of thin superconducting coatings by means of ultra-high vacuum arc facilities
May 24, 2007	S. Tazzari, Tor Vergata Uni, INFN-Roma 2, Rome, Italy, INFN-Roma 2, Rome, Italy	IEEE Symp. on Photonics and Electronics, Wilga, Poland; http://wilga.ise.pw.edu.pl	Ultra pure metal coatings for superconducting applications using the arc in ultra-high vacuum technique
May 24, 2007	J. Lorkiewicz, Tor Vergata Uni., INFN-Roma 2, Rome, Italy	IEEE Symp. on Photonics and Electronics, Wilga, Poland; http://wilga.ise.pw.edu.pl	Recent achievements in ultra-high vacuum arc deposition of superconducting Nb layers
May 24, 2007	R. Nietubyc, IPJ, Swierk, Poland	IEEE Symp. on Photonics and Electronics, Wilga, Poland; http://wilga.ise.pw.edu.pl	Analysis of structure of superconducting Nb layers by means of X-ray techniques
May 24, 2007	P. Strzyzewski, IPJ, Swierk, Poland	IEEE Symp. on Photonics and Electronics, Wilga, Poland; http://wilga.ise.pw.edu.pl	Ultra-high vacuum cathodic arc for deposition of superconducting lead photo-cathodes
June 25-29, 2007	C. Pagani (INFN/LASA, Segrate (MI)),	22 nd PAC Conference 2007, USA	Improved Design of the ILC Blade-Tuner for Large Scale Production, (poster WEPMN020)
June 25-29, 2007	K. Przygoda /DMCS-TUL	22 nd PAC Conference 2007, USA	FPGA-Based Control System For Piezoelectric Stacks Used For SC Cavity's Fast Tuner (poster WEPMN052)
June 26, 2007	P. Strzyzewski, IPJ, Swierk, Poland	IPJ Symp. Warsaw, Poland; http://ipj.gov.pl	Plasma technologies (in Polish)
Sept, 11, 2007	M.J. Sadowski, IPJ, Swierk, Poland	EUROCON 2007, Warsaw, Poland; https://eurocon2007.isep.pw.edu.pl	Deposition of thin metal films by means of arc discharges under ultra-high vacuum conditions
Sept, 11, 2007	R. Russo, Istituto di Cibernetica, CNR and INFN-Na, Naple, Italy	EUROCON 2007, Warsaw, Poland; https://eurocon2007.isep.pw.edu.pl	Deposition and characterization of niobium films for SRF cavity application
Sept 18, 2007	R. Nietubyc, IPJ, Swierk, Poland	CARE SRF Annual Meeting 2007, Warsaw, Poland; https://indico.desy.de/contributionDisplay.py?contribId=1&confId=438	Research and development of superconducting radio-frequency technology for accelerator application (WP4.1)
Sept 18, 2007	R. Russo, Istituto di Cibernetica, CNR and INFN-Na, Naple, Italy	CARE SRF Annual Meeting 2007, Warsaw, Poland; https://indico.desy.de/contributionDisplay.py?contribId=1&confId=438	Recent development in deposition of niobium films by UHVCA in SRF cavity (WP4.2)
Sept. 26, 2007	R. Nietubyc, IPJ, Swierk, Poland	7th Polish Meeting on Synchrotron Radiation Users, Poznan, Poland; http://www.fizyka.amu.pl/ksups	Deposition of superconducting niobium films inside RF-cavities of particle accelerators

6. List of Publications

CARE- pub			
	Quality measurement of niobium thin films for Nb/Cu superconducting RF cavities	R. Russo	Meas. Sci. Technol. 18 (2007) 2299-2313 CARE-Pub-07-009
	Ultra high vacuum cathodic arc for deposition of superconducting lead photo-cathodes	P. Strzyzewski, J. Langner, M.J. Sadowski, J. Witkowski, J. Sekutowicz	Probl. Atom. Sci. & Techn. 1 (2007) Ser. PP 13 , p.185-187 CARE-pub-07-010
	Purity of Nb and Pb films deposited by an ultra-high vacuum cathodic arc	J. Langner, M.J. Sadowski, P. Strzyzewski, J. Witkowski, S. Tazzari, L. Catani, A. Cianchi, J. Lorkiewicz, R. Russo, J. Sekutowicz, T. Paryjczyk, J. Rogowski	IEEE Trans. Plasma Sci. (2007) – in print CARE-Pub-07-006
	Recent achievements in ultra-high vacuum arc deposition of superconducting Nb layers	L. Catani, A. Cianchi, D. Digiovanale, R. Polini, S. Tazzari, J. Lorkiewicz, M.J. Sadowski, P. Strzyzewski, B. Ruggiero, R. Russo	SPIE Trans. (2007) – submitted for publication CARE-Pub-07-007
	Production of thin metallic films by means of arc discharges under ultra-high vacuum conditions	P. Strzyzewski, M.J. Sadowski, R. Nietubyc, K. Rogacki, W. Paszkowski, T. Paryjczak, J. Rogowski	Material Science – Poland (2007) - submitted for publication CARE-Pub-07-008
	Measurement and control of field in RF GUN at FLASH	A. Brandt, M. Hoffmann, W. Koprek, P. Pucyk, S. Simrock, K T. Pozniak, R.S. Romaniuk	Proc. of SPIE Vol 6937 693714, pp.1-11 (2007)
	Radiation measurement in the environment of FLASH using passive dosimeters	B. Mukherjee, D. Rybka, D. Makowski, T. Lipka, S. Simrock	Measurement Science and Technology 18 No 8 (August 2007), pp. 2387-2396
	Application of Low Cost Gallium Arsenide Light Emitting Diodes as KERMA Dosimeter and Fluence Monitor for High Energy Neutrons,	B. Mukherjee, S. Simrock, D. Rybka, R. Romaniuk, J. Khachan	Advance Access published on May 21, 2007
	Superconducting cavity control based on system model identification	Tomasz Czarski	Meas. Sci. Technol. 18 (2007)
	FPGA technology application in a fast measurement and control system for the TESLA superconducting cavity of a FLASH free electron laser	Krzysztof T Pozniak	Meas. Sci. Technol. 18 (2007)

	FPGA-based implementation of a cavity field controller for FLASH and X-FEL	Przemyslaw Fafara, Wojciech Jalmuzna, Waldemar Koprek, Krzysztof Pozniak, Ryszard Romaniuk, Jaroslaw Szewinski, and Wojciech Cichalewski	Meas. Sci. Technol. 18 (2007)
	Measurements for low level RF control systems	S Simrock	Meas. Sci. Technol. 18 (2007)
	New method for beam induced transient measurement	P Pawlik, M Grecki, S Simrock and A Napieralski	Meas. Sci. Technol. 18 (2007)
	Measurement of static force at liquid helium temperature	P Sekalski, A Napieralski, M Fouaidy, A Bosotti and R Paparella	Meas. Sci. Technol. 18 (2007)
	Characterization and compensation for nonlinearities of high-power amplifiers used on the FLASH and XFEL accelerators	W Cichalewski and B Koseda	Online at stacks.iop.org/MST/18/2372
	Radiation monitoring system for X-FEL	D Makowski, B Mukherjee, S Simrock, G Jablonski, A Napieralski and M Grecki	Online at stacks.iop.org/MST/18/2397
	SEU-tolerant IQ detection algorithm for LLRF accelerator system	M Grecki	Meas. Sci. Technol. 18 (2007)
	Effective removal of field-emitting sites from metallic surfaces by dry ice cleaning	A. Dangwal, G. Müller, D. Reschke, K. Floettmann, X. Singer	JOURNAL OF APPLIED PHYSICS 102 , 044903_2007

Conf	Deposition of thin superconducting coatings by means of ultra-high vacuum arc facilities	<u>M.J. Sadowski</u> , P. Strzyzewski, S. Tazzari	16th Symp. on Application of Plasma Proc., Podbanske (Slovakia) CARE-Conf-07-024-SRF .
	Production of thin metallic layers by a technique of arc discharge under UHV conditions – in Polish	<u>P. Strzyzewski</u> , R. Nietubyc, M.J. Sadowski	1st Nat. Conf. Nanotechnology, Wroclaw, Poland May 2007, p.218
	Ultra pure metal coatings for superconducting applications using the arc in ultra-high vacuum technique	A. Cianchi, L. Catani, D. DiGiovenale, J. Lorkiewicz, R. Polini, M.J. Sadowski, R. Russo, B. Ruggiero, P. Strzyzewski, S. Tazzari	IEEE Symp. on Photonics and Electronics, Wilga, Poland, May 2007 http://wilga.ise.pw.edu.pl
	Recent achievements in ultra-high vacuum arc	S. Tazzari, R. Russo, D. DiGiovenale, J.	IEEE Symp. on Photonics and http://wilga.ise.pw.edu.pl
	Analysis of structure of superconducting Nb	<u>R. Nietubyc</u> , P. Strzyzewski, M.J. Sadowski	IEEE Symp. on Photonics and http://wilga.ise.pw.edu.pl

Ultra-high vacuum cathodic arc fro deposition of superconducting lead photo-cathodes	<u>P. Strzyzewski</u> , R. Nietubyc, M.J. Sadowski, J. Witkowski, J. Sekutowicz, S. Tazzari, A. Cianchi, L. Catani, R. Russo	IEEE Symp. on Photonics and Electronics, Wilga, Poland, May 2007 http://wilga.ise.pw.edu.pl
Plasma technologies – in Polish	<u>P. Strzyzewski</u>	IPJ Symp., Warsaw, Poland, June 07 http://ipj.gov.pl
Deposition and characterization of niobium films for SRF cavity application	L. Catani, A. Chianchi, D. DiGiovenale, J. Lorkiewicz, V. Merlo, R. Polini, R. Russo, M.J. Sadowski, M. Saltato, P. Strzyzewski, S. Tazzari	EUROCON 2007, Warsaw (Poland), 9-12 September 2007 CARE-Conf-007-022--SRF
Deposition of thin metal films by means of arc discharges under ultra-high vacuum conditions	<u>M.J. Sadowski</u> , P. Strzyzewski, R. Nietubyc	IEEE EUROCON 2007, Warsaw (Poland), 9-12September 2007 CARE-Conf-007-021-SRF
Improved Design of the ILC Blade-Tuner for Large Scale Production,	C. Pagani, A. Bosotti, N. Panzeri (INFN/LASA, Segrate (MI)),	PAC07, Albuquerque (USA) CARE-Conf-07-025-SRF
FPGA- Based Control System For Piezoelectric Stacks Used For Sc Cavity's Fast Tuner	P. SękalSKI, K. Przygoda, A. Napieralski, W. Jałmużna, S. Simrock, L. Lilje, R. Paparella,	22 nd PAC Conference, June 25-29, 2007, USA
A Novel Approach for Hardware Implementation of a Detuning Compensation Control System for SC Cavities	K. Przygoda (Tech. Univ. Lodz , POLAND), R. Paparella (Univ. degli Studi di Milano, ITALY)	MIXDES 2007
In Situ Measurement of Neutron and Gamma Radiation Exposures During Intercontinental Flights Using Electronic Personal Dosimeter and Bubble Detectors	B. Mukherjee, D. Makowski, V. Mares, D. Rybka, S. Simrock	MIXDES 2007
Integral Interface - Universal Communication Interface for FPGA-based Projects,	A. Piotrowski, S. Tarnowski, G. Jabłoński, A. Napieralski	MIXDES 2007
Low-latency Implementation of Coordinate Conversion in Virtex II Pro FPGA,	G. Jabłoński, K. Przygoda	MIXDES 2007
RadTest - Testing Board for the Software Implemented Hardware Fault Tolerance Research	A. Piotrowski, D. Makowski, S. Tarnowski, A. Napieralski	MIXDES 2007
Sinusoidal Signal Synthesis from Vector Values with Small Quantity of Samples,	S. Tarnowski, A. Piotrowski, A. Napieralski	MIXDES 2007

	Linearization of downconversion for IQ detection purposes	M. Grecki, W. Koprek, S. Simrock	PAC 2007
	Performance of the New Master Oscillator and Phase Reference System at FLASH	S. Simrock, M. Felber, Markus. Hoffmann, Matthias Hoffmann, H. C. Weddig	PAC 2007
	Radiation Field Unfolding at the Free Electron Laser in Hamburg (FLASH) using a Genetic Algorithm	B. Mukherjee, M. Valentan, D. Makowski, D. Rybka, S. Simrock	Eurocon 2007 (in printing)
	A Concept of Irradiation Experiments System	D. Rybka, S. Korolczuk, B. Mukherjee, R. Romaniuk	
	Characterization At Cryogenic Temperatures Of Piezostacks Dedicated To Fast Tuners For Srf Cavities	M. Fouaidy, G. Martinet, N. Hammoudi, F. Chatelet, A. Olivier	Mixed 2007, Ciechocinek (Poland), 21-23 June 2007 CARE-Conf-07-006-SRF
	Status of the Electron Beam Transverse Diagnostics with optical Diffraction Radiation at FLASH	E. Chiadroni, M. Castellano, A. Chianchi, K. Honkavaara, G. Kube	Desy FLASH Seminar, Hamburg June 5, 2007
	Non-Intercepting Electron Beam Transverse Diagnostics with Optical Diffraction Radiation At The Desy FLASH Facility	E. Chiadroni, M. Castellano, A. Chianchi, K. Honkavaara, G. Kube, V. Merlo, F. Stella	PAC07 Conference, Albuquerque 25-29 Juni 2007 CARE-Conf-07-023-SRF
	Piezo-assisted blade tuner: cold test results	C.Pagani, A.Bosotti, N.Panzeri, R.Paparella, P.Pierini, C Albrecht, R.Lange, L.Lilje	SRF07, Beijing (China) CARE-Conf-07-026-SRF
	MatLab script to C code converter for embedded processors of FLASH LLRF control system	K.Bujnowski, A.Siemionczyk, P.Pucyk, J.Szewiński, K.T.Poźniak, R.S.Romaniuk	Proc. of SPIE Vol 6937 693723, pp.1-8 (2007)
	Decomposition of MATLAB script for FPGA implementation of real time simulation algorithms for LLRF system in European XFEL	K. Bujnowski, P.Pucyk, K. T. Pozniak, R. S. Romaniuk	Proc. of SPIE Vol 6937 693724, pp.1-12 (2007)
	Multi-cavity complex controller with vector simulator for TESLA technology linear accelerator	Tomasz Czarski, Krzysztof T. Pozniak, Ryszard S. Romaniuk, Jaroslaw Szewinski	Proc. of SPIE Vol 6937 693716, pp.1-9 (2007)
	FPGA control utility in JAVA	Paweł Drabik, Krzysztof T. Pozniak	Proc. of SPIE Vol 6937 693725, pp.1-9 (2007)
	Data acquisition module implemented on PCI Mezzanine card	Lukasz Dymanowski, Rafal Graczyk, Krzysztof T. Pozniak, Ryszard S. Romaniuk	Proc. of SPIE Vol 6937 693719, pp.1-9 (2007)

	Copper TESLA structure - measurements and control	Jakub Główka, Mateusz Maciaś	Proc. of SPIE Vol 6937 693727, pp.1-11 (2007)
	FPGA systems development based on Universal Controller Module	Rafał Graczyk, Krzysztof T. Poźniak, Ryszard S. Romaniuk	Proc. of SPIE Vol 6937 693721, pp.1-8 (2007)
	FPGA based PCI Mezzanine card with digital interfaces	Kamil Lewandowski, Rafał Graczyk, Krzysztof T. Poźniak, Ryszard S. Romaniuk	Proc. of SPIE Vol 6937 693718, pp.1-9 (2007)
	Vector modulator board for X-FEL LLRF system	M. Smelkowski, P.Strzalkowski, K.T.Pozniak	Proc. of SPIE Vol 6937 693720, pp.1-8 (2007)
	Versatile LLRF platform for FLASH laser	Paweł Strzałkowski, Waldemar Koprek, Krzysztof T. Poźniak, Ryszard S. Romaniuk	Proc. of SPIE Vol 6937 693717, pp.1-10 (2007)
	High precision SC cavity alignment measurements with higher order modes	Stephen Molloy, Josef Frisch, Douglas McCormick, Justin May, Marc Ross, Tonee Smit1, Nathan Eddy, Sergei Nagaitsev, Ron Rechenmacher, Luciano Piccoli, Nicoleta Baboi, Olaf Hensler, Lyudvig Petrosyan, Olivier Napoly, Rita Paparella and Claire Simon	2007 IOP Publishing Ltd

CARE Report	Full Characterization of Piezoelectric Actuators used for Superconducting RF Cavities Fast Active Tuning	M. Fouaidy, G. Martinet, N. Hammoudi, F. Chatelet,	Deliverable 8.4.8: Report on IN2P3 tuner activities CARE-Report-2007-015-SRF
--------------------	--	--	--

CARE Note	Radiation hardness tests of piezoelectric actuators with fast neutrons at liquid helium temperature	M. Fouaidy, G. Martinet, N. Hammoudi, F. Chatelet, A. Olivier, S. Blivet, F. Galet	
	Lorentz detuning compensation of a 9-cell TTF cavity with the integrated piezo tuner at Saclay	G. Devanz, P. Bosland, M. Desmons, E. Jacques, M. Luong, B. Visentin, M. Fouaidy	CARE-Note-2007-011-SRF

CARE/SRF Document	Sports car treatment for cavities	Barbara Warmbein	ILC NewsLine 24 May 2007
	Radiation issues in the single tunnel environment	M. Grecki	
	Status of R&D at DESY	Waldemar Koprek	

PhD Thesis	"Diagnostic System for Backing Calorimeter and Low Level RF of VUV-FEL"	Tomasz Jezynski	http://flash.desy.de/sites/site_vuvfel/content/e403/e1869/e1870/e1875/infoboxContent1878/Jezynski_PhD.pdf
	"Smart Materials as Sensors and Actuators for Lorentz Force Tuning System"	Przemyslaw Sekalski	http://flash.desy.de/sites/site_vuvfel/content/e403/e1869/e1870/e1875/infoboxContent1876/Sekalski_PhD.pdf
	"RF field amplitude and phase calibration for particle accelerator based on beam induced transient detection"	Pawel Pawlik	http://flash.desy.de/sites/site_vuvfel/content/e403/e1869/e2241/e2243/infoboxContent2244/PawelPawlikthesis-ebook.pdf
	"Enhanced Field Emission from Metallic Surfaces and Nanowires"	Arti Dangwal	Wuppertal 2007, WUB-DIS 2007-08

Master Thesis	"Visualization of Systems Applied to FSM Control"	Piotr Cieciora	http://flash.desy.de/sites/site_vuvfel/content/e403/e1869/e1870/e1871/infoboxContent1874/Cieciora_MSc.pdf
	"Design of Radiation Tolerant Integrated Circuits"	Pawel Malinowski	http://flash.desy.de/sites/site_vuvfel/content/e403/e1869/e1870/e1871/infoboxContent1872/Malinowski_MSc.pdf
	"Timing Definition Language for POSIX environment"	Maciej Borzecki	http://flash.desy.de/sites/site_vuvfel/content/e403/e1869/e1870/e1871/infoboxContent1873/Malinowski_MSc.pdf
	"Redundancy as a way of improving software reliability"	Maciej Borzęcki	
	"Design of radiation tolerant microcontroller implemented in FPGA"	Julian Waldek	
	"Implementation of XML configuration manager for Distributed Finite State machines of VUV-FEL"	Piotr Przybylak	
	"Integrated Radiation Sensor"	Ewa Jędrzejowska,	
	"Design of Radiation Tolerant Transmission Channel Circuit;	Jakub Mielczarek	http://flash.desy.de/sites/site_vuvfel/content/e403/e1869/e1879/e1880/infoboxContent1881/Mielczarek_MSc.pdf
	"Distributed System for Designing Reliable Digital Systems Using Genetic Algorithms"	Tomasz Norek	http://flash.desy.de/sites/site_vuvfel/content/e403/e1869/e1879/e1880/infoboxContent1882/Norek_MSc.pdf
	"Software Implementation of Mechanisms Improving The Reliability of DSP Systems in The Radioactive Environment"	Marcin Wojtczak	http://flash.desy.de/sites/site_vuvfel/content/e403/e1869/e1879/e1880/infoboxContent1883/Wojtczak_MSc.pdf

7. Report of the International Advisory Committee

This is the final report of the Annual Review (September 2007) held by the International Advisory Committee of the activities performed by the JRA1 project of Coordinated Accelerator Research in Europe (CARE)

The following members of the IAC were present: H. Padamsee (Chair), P.Kneisel, W. Weingarten, I. Campisi.

Executive Summary

The CARE team and its management deserve congratulations on successfully completing a large number of work packages with a variety of goals. There is good progress on remaining work, as detailed in the remarks of the IAC members attached. This is especially commendable since the CARE faces competition for the same resources as for XFEL and ILC work. The publication and report output has been impressive. The communications between groups has improved as for example between those responsible for EP parameter studies and EP modeling, spinning and hydro-forming, field emission scanning and dry ice cleaning.

The committee recognizes important success in the seamless cavity arena. Challenges for hydro-forming and spinning have shown many common elements, and the two groups have learnt valuable lessons from each other. Several 3-cell Nb cavities have been spun with new machinery installed. Three 3-cell cavities have been hydro-formed and a 9-cell completed from same units. For Vacuum Arc Thin Film Deposition the film characterizations show properties closer to bulk niobium compared to thin films deposited by sputtering technique. There has been continuing progress in eliminating droplets. Two facilities are ready for coating copper cavities, although aggressive HPR has removed the film in places. For electropolishing studies, automated systems have been installed at two locations and interesting results have emerged from EP modeling. The Dry Ice Cleaning team has completed Installations for cleaning single cells and the gun. Several single cell Nb cavities have been tested with encouraging results for suppressing field emission. In tandem, DC scanning of samples show fewer emitter with dry ice cleaning versus the customary high pressure water rinsing. Dry ice cleaning has the long term potential to clean fully assembled cavities.

The IAC makes the following recommendations. The remaining time to finish is short, and there are many attractive paths being pursued. Many activities have arrived at an advanced stage that an emphasis on performance testing is now desirable over continued development of any particular approach. We recommend the management to pick select areas ripe for testing. For example, it may be appropriate to test successfully spun 3-cell cavities after treatment, over fabrication of one 9-cell unit. Similarly, test the first 9-cell hydro-formed cavity over fabrication of a second 9-cell. In vacuum arc film deposition, apply best copper cleaning methods known from past sputtering activities. After coating, test one copper coated cavity (from each facility) first without HPR, then gradually increase pressure for HPR, (rather than coat many cavities at once.) In the electropolishing arena, apply automated EP systems installed at DESY and Saclay to several single cell cavities to determine impact on reproducibility rather than investigate recipe variations.

We recognize that there is strong competition for preparation and testing resources. By defining such specific tasks it may become possible to take many work packages to final completion.

From what we heard and saw we are confident of the broad impact of CARE progress on world-wide SRF community activities for XFEL and eventually for ILC. Congratulations.

8. Status of Activities

WP 2 Improved component design

The cavity geometry and the design of many components as flanges, HOM, etc. can be kept as present. The proposed changes are related to the end group:

- less expensive Nb,
- cheaper and simplified machining and welding.

We propose to change significantly the connection between the high RRR / low RRR (Nb Reactor Grade, RG) ring, and the NbTi cone. In the existing solution a Nb RG ring is welded to the high RRR Nb ring. Also a stiffening ring is welded from the Nb RG part to the cavity wall. The NbTi cone is welded to the Nb RG part. Our proposal is to change the high RRR part shape and to weld directly the NbTi cone to the high RRR Nb ring. No more low RRR (Nb RG) part and stiffening for the first and last half cell are foreseen. Preliminary calculation done at Milano indicates that these stiffening parts have negligible effect on the cavity. Fig. 2.1 shows the proposed solution compared with the existing one.

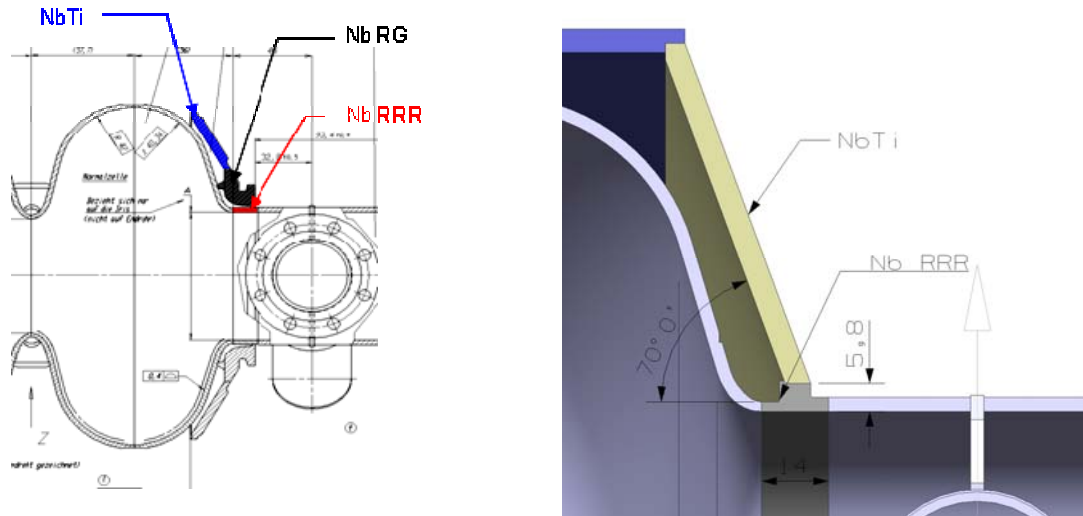


Fig. 2.1: Existing and proposed solution

All the other parts of the end group are kept unchanged. Proper machining on the Nb high RRR part will help the welding and the alignment of the NbTi cones. In case of need of a reference surface for the cavity alignment, this can be tack welded on the NbTi cone.

The assembly procedure for the final welds (adjustment of the He tank length) can be optimized for an easier and cheaper procedure by means of proper surface machining as in fig. 2.2.

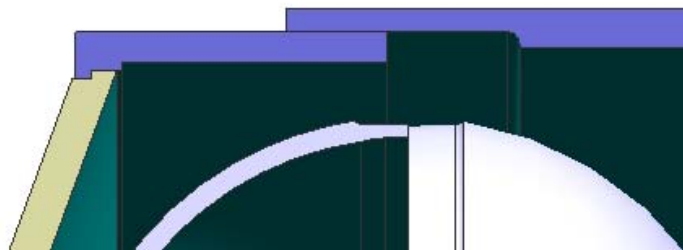


Fig. 2.2: Detail of the Ti He Tank adjustment ring welded to the NbTi cone.

No bellow is foreseen at the He tank extremities: we propose to use the coaxial tuner which has bellow in the center. As a consequence, all the machining for the Saclay tuner can be totally avoided. Using the blade tuner, the magnetic shielding can be located either between the He tank and the Coax tuner or inside the tank.

A preliminary evaluation of strength and stiffness has been done both on the present geometry and on the proposed one. The differences are reported in the next figures.

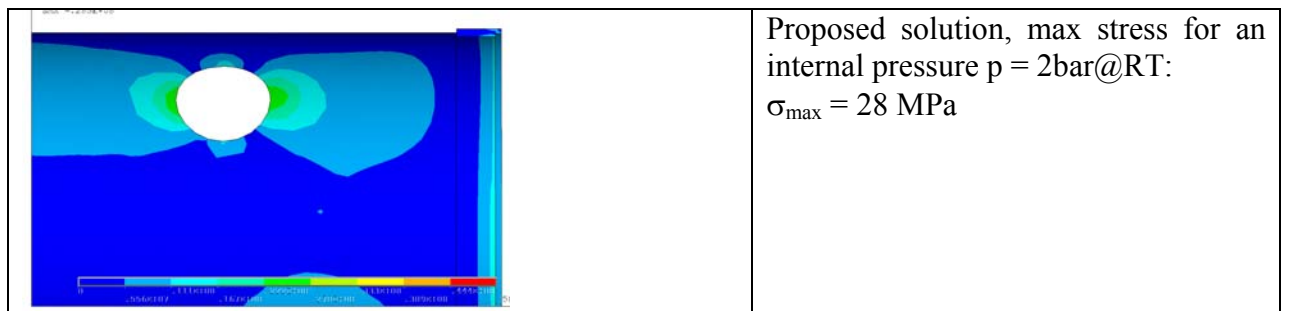
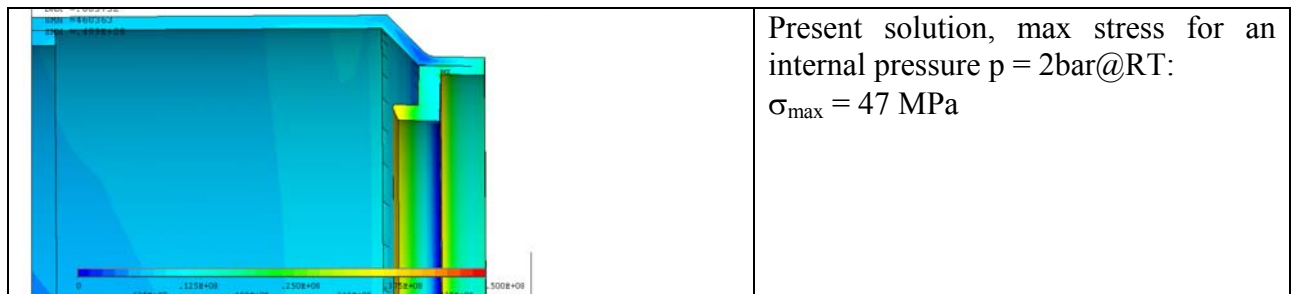
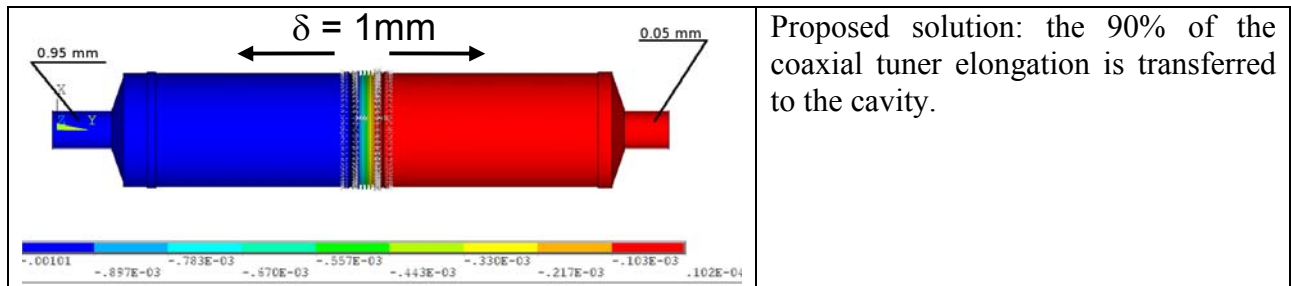
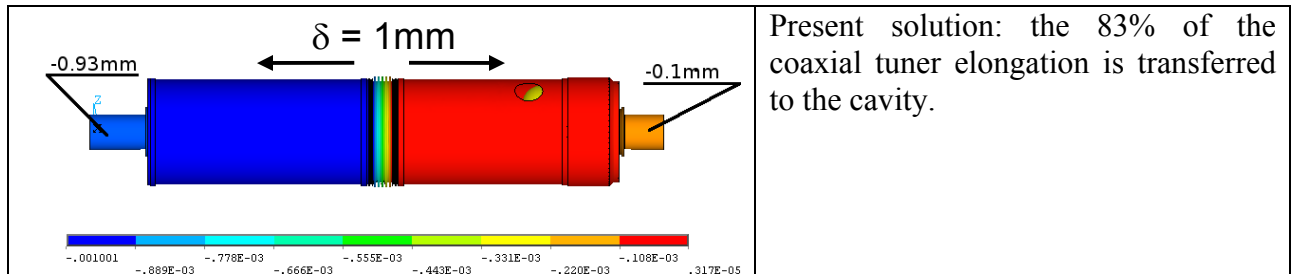


Fig. 2.3: Comparison between new and old LHe tank design

Concerning the electron beam welding, we are collecting information about EB welding machines in companies and laboratories. We asked companies and labs to send details concerning the available EBW machines (model, power), the vacuum chamber (dimensions, volume), the working plane (linear and rotary motions), the electron beam (accelerating voltage, beam current), vacuum system (type of pumps, vacuum cycle time, diagnostics, venting gas), and any useful comments. In some case data were available only on the WEB.

The collected information is summarized in Tab. 1.

laboratory / firm	E.B. Machine				max comp. dim.			working plane		Motion	beam			vacuum				Welding info and comments	
	machine	model	power	chamber volume	diam	length	weight	linear motion	rotary motion	Oil Free / in vacuum motors and gears	rotary motion	V (kV)	I (mA)	Pumps	Diagnostics (Residual gas analysis)	Vacuum cycle time	Gas used for venting	welding seam depth	comments
ACCEL			30 kW	10 m ³	1200mm	3500mm	up to 4Mp									10 ⁻⁵ mbar			data available only on the WEB: http://www.accel.de/_struktur/manufacturing_technologies.htm
ACCEL			7.5 kW	1.4 m ³	300mm 500mm	5000mm 1350mm	up to 250kp									10 ⁻⁵ mbar			
CERCA AREVA	TECHMETA	CT4	15 kW	8 m ³	1500 mm	4500 mm	1000 Kg	x = 1500 mm y = 500 mm	>360°	yes	no	60	250	Cryogenic	yes	10 ⁻⁵ mbar in 15' 10 ⁻⁶ mbar in 5h	Pure Argon		direct information from the company
	SCIACKY	Internal	6 kW									30	200						
ZANON	PTR	EBW 8001/30-150 CNC	15 kW	8 m ³	1200 mm	1500 mm	2000 kg	CNC control X=1100mm Y=550 mm	CNC control	yes	dynamic and static	150	200	mechanical + diffusion pump	no	15' for 8x10 ⁻⁴ 120' for 4x10 ⁻⁵	Air	min.0.4 mm max.120 mm	direct information from the company
DESY	Steigenwald	150 keV	15 kW	7.4 m ³	1400 x 1600	3300		1400 mm	yes	yes	5°	150	100	Cryogenic	yes	30'	Nitrogen		
Jlab	Sciaky	VX4		6.4 m ³				6 axis of motion (x,y,z, rotation, tilt of rotation,gun tilt)				60	700	Cryogenic	no	12'	Nitrogen		
FZJ	ZAT	K40-G150KM	15 kW	4 m ³				960 x 590 mm				170		Oil free					

Tab. 1: Electron beam welding parameters information from companies and labs

WP 3 Seamless Cavity Production (SCP)

Task 3.1 Seamless cavity production by spinning

The spinning lathe has been successfully set up for the multi-cells fabrication. A new procedure for getting the thickness uniform all over the cavity wall has been developed. The new method combines spinning operation with the upsetting technique. In other words, the uniform thickness is obtained by increasing the pressure between late tailstock and headstock meanwhile spinning. More simply, by shrinking the cavity across the cavity length, meanwhile the roller presses the Niobium along the equator radius in order to get more Nb material to the iris. This method permits a good wall thickness uniformity along the eight irises and the nine neighboured equators, as sketched in the following picture.

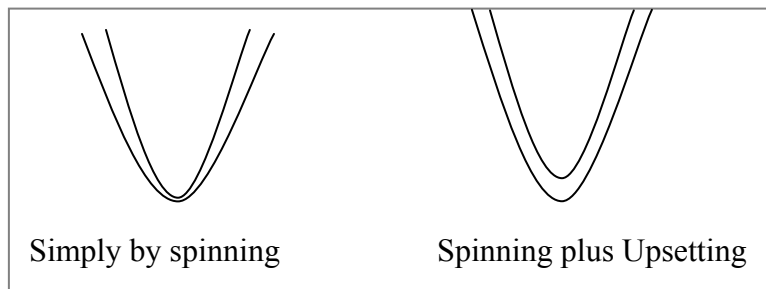


Fig. 3.1: Constant wall thickness is established by a combination of spinning and upsetting technique

However a problem appears in the two end-halfcells close to the cut-off tubes, just the one where this method is not applicable. There is indeed a narrow circle where the wall thickness is thinner and this is just in the halfcell-tube conjunction. This problem was experienced when tumbling a multicell cavity, as shown in the following picture. The thinner wall between halfcell and tube was immediately consumed by the abrasive action of silicon carbide media so that the beam pipe was “cut” from the cavity body.



Fig. 3.2: Destroyed cavity after tumbling because of a too small wall thickness at the iris region
The thickness uniformity experimentally found in this region is sketched in the next figure.

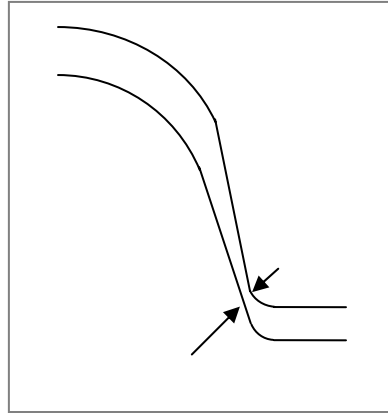


Fig. 3.3: Measured wall thickness after fabrication of a Nb cavity by spinning

In order to try to solve this problem, we are currently building a further collapsible die to add to the collapsible mandrel. The added mandrel part has the shape of a frustum and it follows the scheme sketched below.

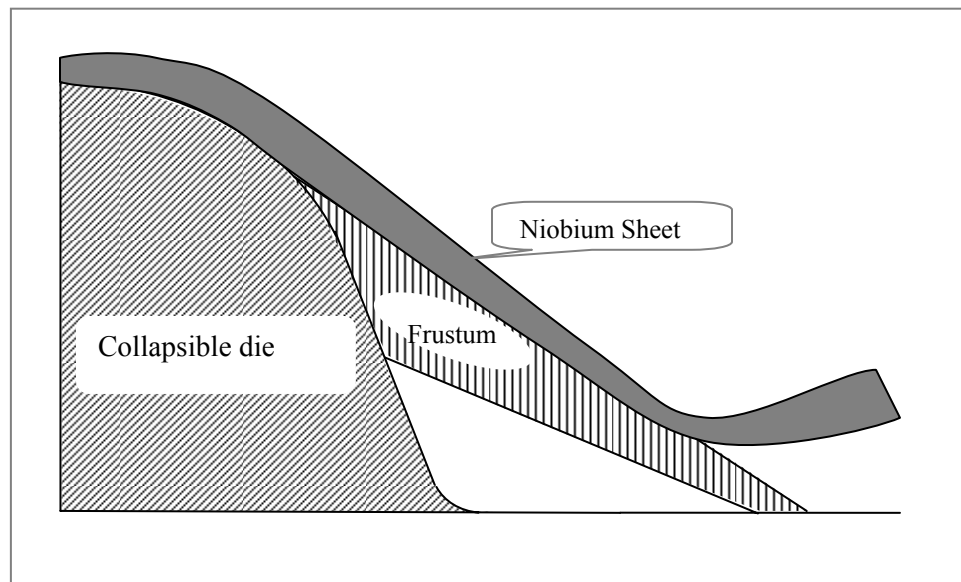


Fig. 3.4: Prinzipal layout of the modified tool in order to avoid the thinning of the Nb wall near to the iris location

The optimization of this new tool is in progress. After this a new series of cavity production by spinning will be started.

Task 3.2 Seamless cavity production by hydroforming

Several three 3-cell units have been fabricated by hydroforming from seamless tubes (ID 150mm, wall thickness 3 mm). After necking the hydroforming was performed in two stages in order to achieve the correct shape, uniform wall thickness of the complete cavity and to suppress possible instabilities in the tube expansion process.

Completing of a worldwide first 1.3 GHz nine cell seamless resonator (without equator welds) is done at the company ZANON.

Completion included following steps (see Fig. 3.5):

- Fabrication of the long and short end groups connected with three cell units
- Machining, preparation and welding of three units together in a 9 cell cavity (two iris welds done from outside)
- Machining, preparation and weld on of the stiffening rings

The completion was successfully done and the seamless resonator has been delivered to DESY (Fig. 3.6).

The cavity is currently in the preparation for the vertical RF test at DESY.

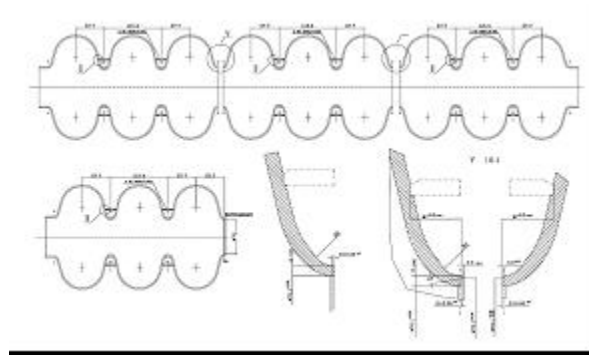


Fig. 3.5: Completion of the hydroformed cavity



Fig. 3.6: Picture of the hydroformed cavity Z14

Thermal Conductivity of Large Grain/Single Crystal Niobium

Bulk niobium cavities made from large grain or single crystal niobium may benefit from the thermal conductivity enhancement at around 1.8K due to reduction of the scattering of phonons on grain boundaries. The total heat conductivity of the superconducting metal is obtained by adding the electron term and the phonon term.

$$\lambda_s(T) = R(y) \left[\frac{\rho_{295K}}{L_0 \cdot RRR \cdot T} + aT^2 \right]^{-1} + \left[\frac{1}{D \exp(y)T^2} + \frac{1}{BIT^3} \right]^{-1} \quad [1]$$

T-Temperature, *RRR*-residual resistivity ratio, *l*-phonon mean free path.

Taking into account the basic data for niobium these parameters are easily calculated:

$$y = \alpha \bullet T_c / T, \quad \alpha = 1.76, \quad L = 2.45 \times 10^{-8} \text{ WK}^{-2}, \quad a = 2.3 \times 10^{-5} \text{ mW}^{-1} \text{ K}^{-1},$$

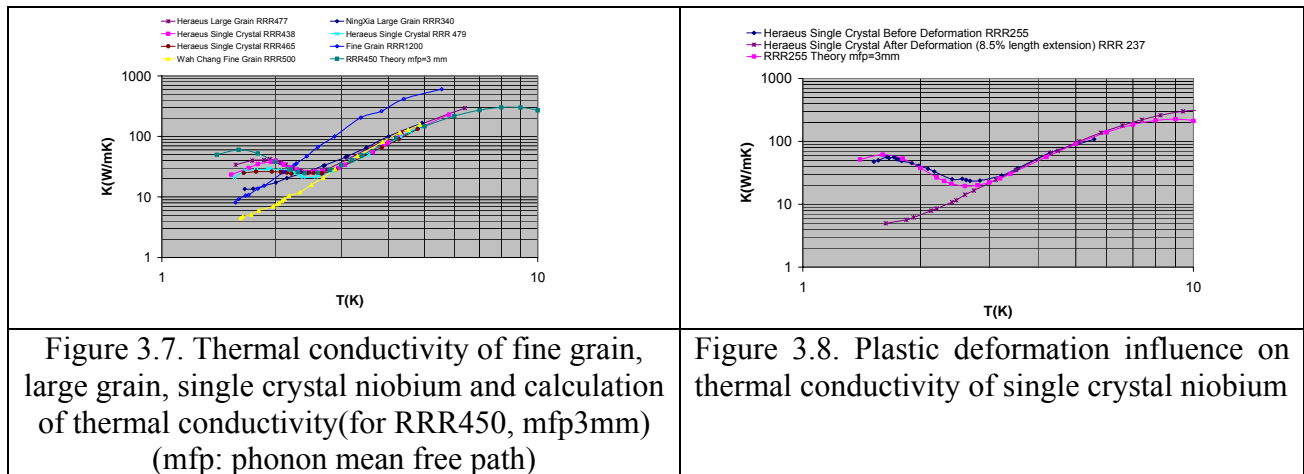
$$1/D = 300 \text{ mK}^{-3} \text{ W}^{-1}, \quad B = 7.0 \times 10^3 \text{ Wm}^{-2} \text{ K}^{-4}, \quad G - \text{grain size.}$$

The fitting for high purity niobium coefficients are given in work [1].

Large grain or single crystal Nb material has less grain boundaries as compared to polycrystalline material. Therefore it is expected that the contribution of phonon scattering on grain boundaries will be significantly reduced for these materials. Calculation of thermal conductivity using the formula for $\lambda_s(T)$ and as the phonon mean free path the sample width of ca. 3 mm (instead of grain size for material normally ca. 50 μm) can be seen in Fig. 7-8. Phonon peak is clearly pronounced.

The thermal conductivity of a series of fine grain (polycrystalline), large grain and single crystal niobium samples were measured at low temperatures. The experimental results (Fig. 3.7-3.8) are emphasis pronounced phonon peaks on large grain and single crystal heat treated at 800°C niobium samples produced by W.C. Heraeus (Figure 3.7), while no ‘phonon peak’ on fine grain samples independently on RRR value are observed. The dependence of the phonon peak on crystallographic orientation was not dedicated. Thermal conductivity in the range 4-10 K is consistent with theoretical model.

No “phonon peak” was observed on a large grain niobium sample from Ningxia. Additional crystallographic structure investigation has shown that NINXIA large grains consist of many small powders like crystals.



Further investigation has shown that the phonon peak may be destroyed by stress inside the sample due to plastic deformation. Already at a small plastic deformation of 8.5% the phonon peak totally disappears (Figure 3.8). It implies that the final cavity made with large/single

crystal niobium might not benefit from the thermal conductivity enhancement due to the plastic deformation during cavity fabrication (deep drawing of half cells). In this context final annealing at ca. 800 °C might be helpful not only for outgassing of the hydrogen but also for the stress relaxation.

Further investigation of magnetic, mechanical properties, crystal orientation and structure of large grain and single crystal niobium with the aim to make the fabrication procedure more efficient are in progress.

- [1] Koechlin, F., Bonin, B., Parametrisation of the Niobium Thermal Conductivity in the Superconducting State, *Supercond. Sci. Technol.* 9 (1996) 453-460.

WP 4 - Thin film cavity production

Task WP4.1 – Linear cathode coating

In 2007 the WP4.1 activities were concentrated on the final preparation of the UHV linear arc facility. An improved model of the cylindrical Venetian-type filter with cooling flanges at the both ends has been ordered at an external manufacturer. Due to very critical requirements in regard to the quality of the applied materials (OFHC) the manufacturing met some difficulties and the new filter should be finished after summer holidays. Another filter, designed as a cylindrical set of cooled copper tubes distributed symmetrically, is also under manufacturing and it should be obtained this autumn. The UHV linear-arc facility was equipped with a laminar flow chamber, as shown in Fig. 4.1.

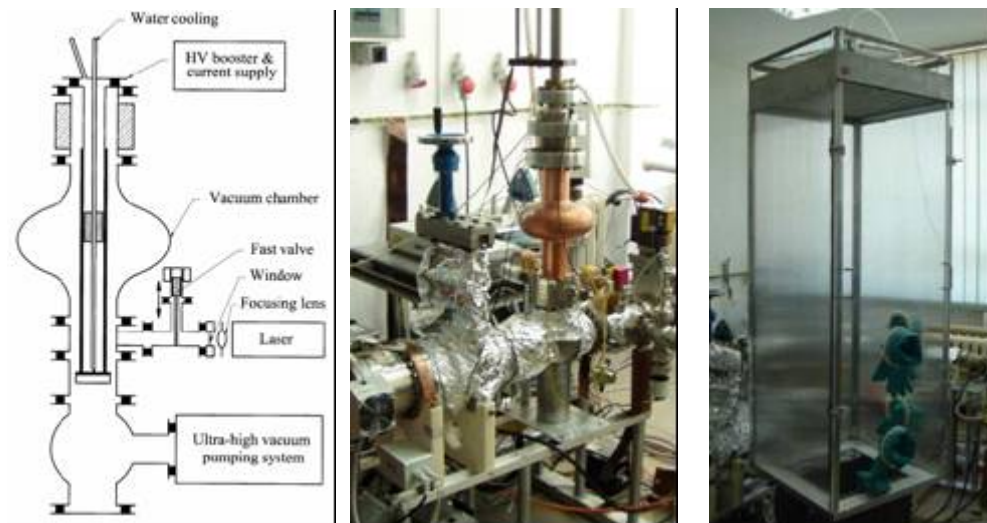


Fig.4.1. Scheme and view of UHV cylindrical-arc facility constructed at IPJ and a removable laminar flow chamber.

Before a delivery the first original 1.3-MHz copper cavity the WP4.1 activities were concentrated on analyses of various samples deposited within the UHV linear-arc facility. An example is shown in Fig. 4.2.

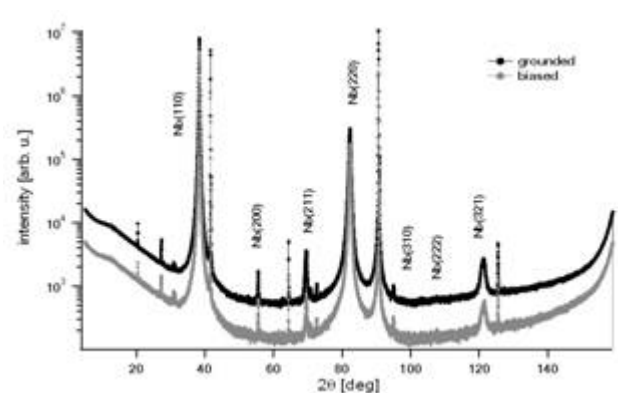


Fig. 4.2. X-ray diffraction patterns from Nb layers deposited upon the biased- and grounded-substrates.

The X-ray diffraction lines from a sapphire substrate and the deposited Nb-film were identified. The lines from the substrate appeared to be stronger and narrower than those from the Nb layer. Estimates of the Nb lattice constant have given values very close to that observed for the bulk Nb crystal.

Simultaneously with the described tests we carried various tests of the samples deposited during previous operational runs. Since the film oxidation may be an important reason for the deterioration of the superconductive properties, the oxidation of Nb/Al₂O₃(0001) samples has been studied in order to identify various niobium oxides formed during the thermal annealing (up to 600 °C) in the atmosphere characterized by the partial pressure of oxygen equal to 10⁻⁴ mbar. Grazing-incidence scans and $\theta - 2\theta$ diffraction patterns have been measured with the Cu K _{α} ,2 radiation for the films before and after their oxidation, as shown in Fig. 4.3.

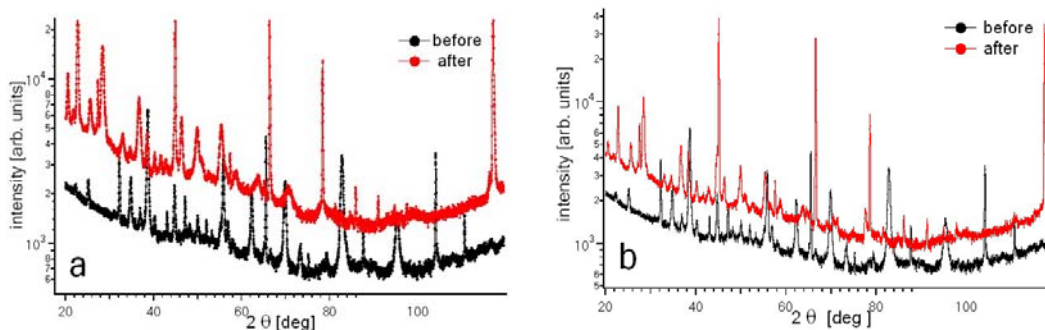


Fig. 4.3. X-ray diffraction patterns of the Nb/Al₂O₃ (0001) film before and after the oxidation: **a** – grazing incidence detector scan, **b** – θ - 2θ pattern.

The obtained results show that the deposited Nb layer can be converted into a new crystalline phase. A detailed analysis of this phase has to be continued because it might be of importance for future deposition processes.

X-ray diffraction measurements were also performed for the Nb/Al₂O₃ samples, using a W2 beam-line at the DORIS storage-ring in DESY. The enhanced 110 reflection at 38.45 ° indicated that the preferable orientation of the 110-plane is parallel to the sample surface. In the θ - 2θ pattern such a reflection showed two (sharp and broadened) components, while only a sharp one was observed in the grazing incidence pattern. The broadened component can be interpreted as a result of a thin (a few nanometers) epitaxial-layer formed on the sapphire substrate directly.

The first original copper cavity was delivered from CEA-Saclay in April 2007, but it was broken during its transport to Poland. After the inspection of that cavity by Dr B. Visentin and Miss M. Bruchon during their visit at IPJ on May 10-11, 2007, it was sent back to CEA-Saclay. The second cavity (with an improved external supports) was delivered from CEA-Saclay in June 2007, and its internal walls were coated with the Nb-layer, as shown in Fig.4.4.



Fig. 4.4. End-on picture of the second cavity from CEA-Saclay, taken after its coating at IPJ.

The coated cavity was sent back to CEA-Saclay in order to perform high-pressure rinsing and RF tests. Unfortunately, it appeared that adhesion of the deposited Nb-layer was too low to withstand the high-pressure rinsing and further deposition tests have to be performed. In order to improve the adhesion during next deposition processes, it has been decided to apply an appropriate biasing of the original cavity by means of an auxiliary anode and/or to perform preliminary ion cleaning. A new auxiliary anode has just been designed and installed within the UHV linear-arc facility for electrical tests and depositions upon some samples are to be performed in June 2007. The next deposition of the original 1.3-MHz copper cavity will be performed when it is delivered from the CEA-Saclay.

The WP4.1 team has received the information from the CEA-Saclay that our Nb/Cu sample, which was deposited within the UHV linear-arc facility at IPJ, had undergone the HPWR procedure and the Nb layer was not destroyed. It is very positive information as regards future experiments.

Task WP4.2 – Planar-Arc Cathode Coating

In 2007 the WP4.2 team activity was mainly devoted to the upgrade of the UHV unfiltered planar arc facility dedicated to single cell deposition tests, aimed at improving the system flexibility, the ion current delivery and the configuration reproducibility. In order to make the film thickness more uniform particularly in the equator region, an external slanted rotating coil

was added to bend the plasma column and rotate it around the cavity axis. A schematic drawing and a view of the modified UHV planar-arc facility are shown in Fig.4.5.

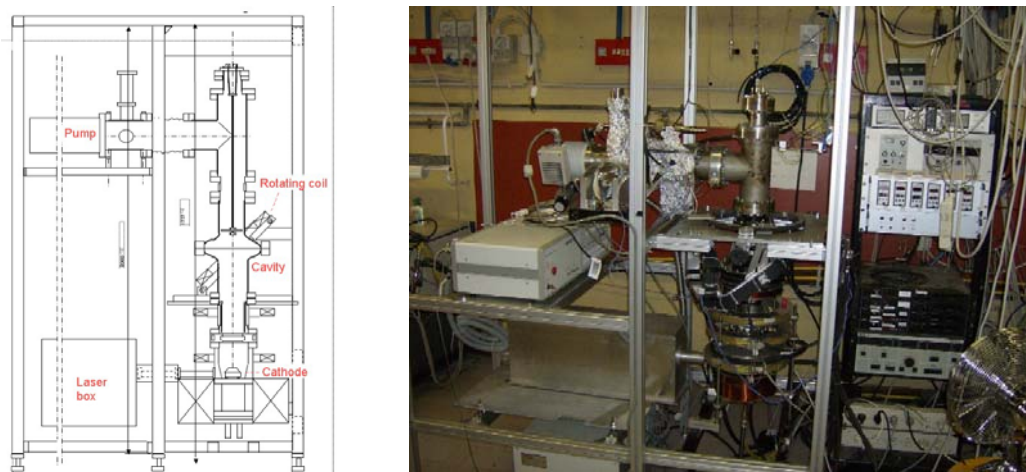


Fig.4.5. Layout of the modified UHV planar-arc system and a picture taken during assembly.

With the upgraded system equipped with a SS dummy cavity carrying a number of ion collectors, it was verified that the deposition rate upon the upper half-cell surface, facing the planar cathode, exceeds that on the bottom half-cell by an order of magnitude, confirming that the cavity must be coated from both sides. The design of such a system, equipped with two cathodes and including micro-droplet filtering, is in progress.

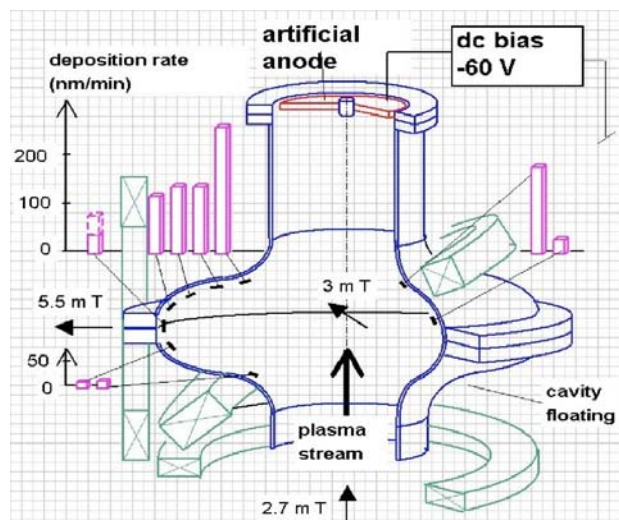


Fig.4.6. Sketch of the SS dummy cavity showing the set of magnetic coils controlling the plasma beam position, the ion collectors arrangement and the measured deposition rates at their locations.

In the meantime, the magnetic field distribution will be further studied in order to further improve the deposition rate in the equator region.

The influence of pulsed bias on the deposition rate was studied by coating, under a number of different conditions, an array of 11 sapphire samples fastened to the dummy cavity inner surface. Measured deposition rates are shown in Fig. 4.7.

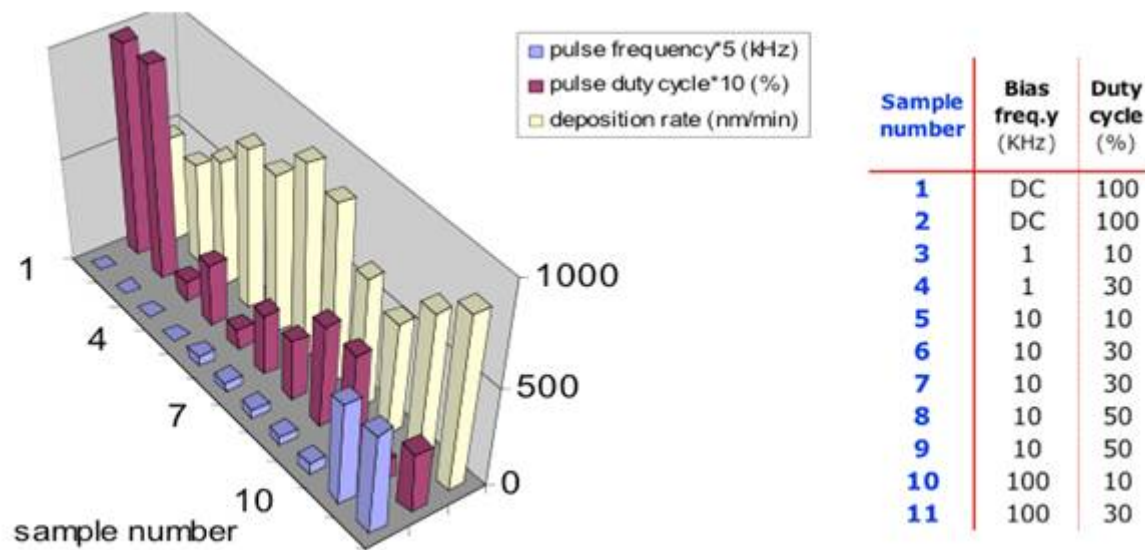


Fig. 4.7. Deposition rates measured at bias voltage of -60 V and different bias pulsing frequencies and duty cycles.

The effects on the film characteristics of pulsed as compared to continuous negative biasing was also investigated for various bias voltages, repetition frequencies and pulse duty factors. Tests on samples have shown that bias pulsing improves the morphological and structural properties of the deposited Nb films. The measured RRR of the best sample was 80. Larger grain sizes (up to microns) and less defects are obtained under the best conditions so far, namely 10 kHz and 30%-50% duty cycle, as shown in Fig. 4.8.

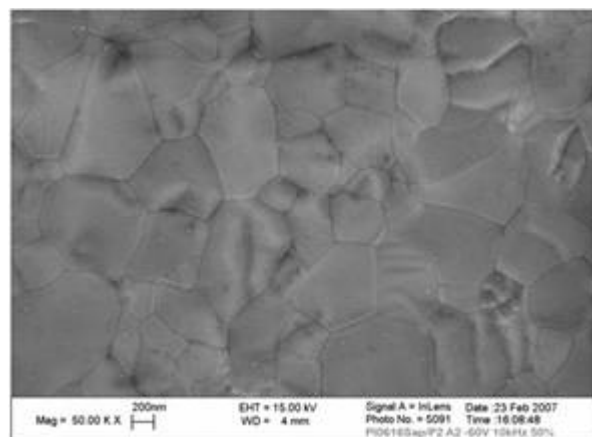


Fig. 4.8. FEG-SEM picture of a $1.4\text{-}\mu\text{m}$ -thick Nb film, deposited on sapphire, with -60 V bias, pulsed at 10 KHz and 50% duty cycle.

During sample depositions an infrared camera has been used to investigate temperature distribution over the whole system and in particular that of the sample substrate. Thermographic pictures, taken through an observation window, showed that the sample holder temperatures ranged from ~ 25 °C to ~ 150 °C. The sample substrate temperature is therefore expected to come close to the 150 °C upper value. Temperature distribution on the cavity walls and on the plasma duct also gave information on the plasma flow: a typical observation is shown in Fig.4.9.

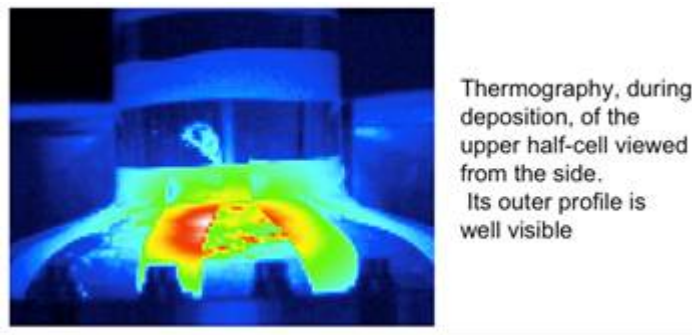


Fig.4.9. Color coded temperatures of the upper dummy half cell during deposition tests.

The first 1.3-MHz copper single cell, prepared for coating and delivered by CEA-Saclay at the end of June 2007, was successfully coated, in the unfiltered system described above, on July 11 and is being sent back to CEA-Saclay for final cleaning and RF measurements. The inner coated surface is shown in Fig. 4.10.

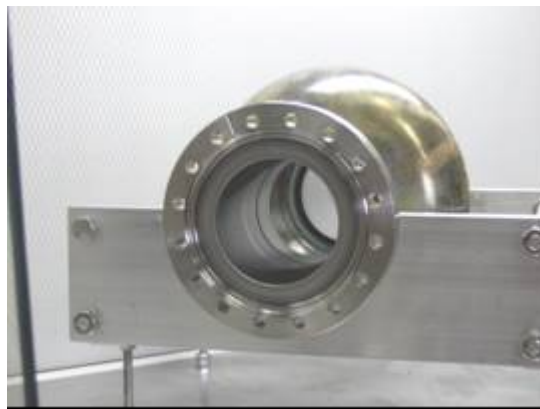


Fig.4.10. The first single cell copper cavity, UHV planar arc coated in Tor Vergata lab.

The milestone “Report on quality of high- T_c material coating“ has not been reached due to the fact that priority was given to the preparation of the UHV planar-arc facility for single cell deposition. It is estimated that the mentioned milestone will not be reached before the end of 2007.

Results of the studies described above have already been reported in several publications and papers presented (or to be presented) at international scientific conferences this year (see the list in this Report).

WP 5 Surface preparation

5.1 EP on single cells

After some modifications the EP system for single cell at Saclay is operating and in use. Fig. 5.1 shows the installation in operation.



Fig. 5.1: Single cell electropolishing (EP) installation at Saclay.

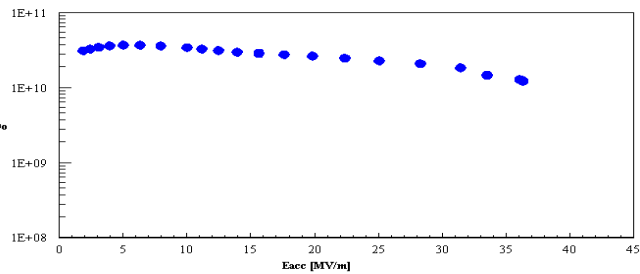


Fig. 5.2: Test result of the first treated cavity at Saclay

In order to calibrate the new EP facility a test cavity was electro-polished according to the EP parameter set under use at the DESY 9-cell EP installation. The performance of this cavity is shown in figure 5.2. An accelerating gradient of 36 MV/m at a quality factor of 1×10^{10} was measured, which is very close to the original treatment and measurement at DESY.

During 2007 a variety of EP mixtures were applied to several single test cavities. Originally these mixtures were developed during a small sample test program in 2006. The cryogenic measurement of the 1-cell cavities could also be done at Saclay because the move and re-installation of the cryogenic plant was finished in 2007. A summary report of the investigation of EP parameter optimisation will be finished early 2008.

5.2 EP on multi cells

The design of new and optimized electrodes has been started. Calculations of the existing electrode are in an acceptable agreement with the parameters found on the DESY EP apparatus even if influences like acid flow speed and temperature variations are not included in the calculation. Various electrode designs are under calculation. One promising design is shown in Fig. 5.3. The main difficulty is to assure a high EP rate at the equator area in comparison to the iris location which is much nearer to the central cathode. Therefore additional radial rods are attached to the horizontal center electrode. The current distribution with and without these rods are calculated and shown in figures 5.4.

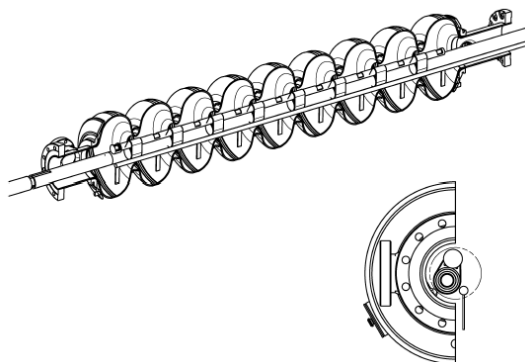


Fig. 5.3: Optimised electrode shape

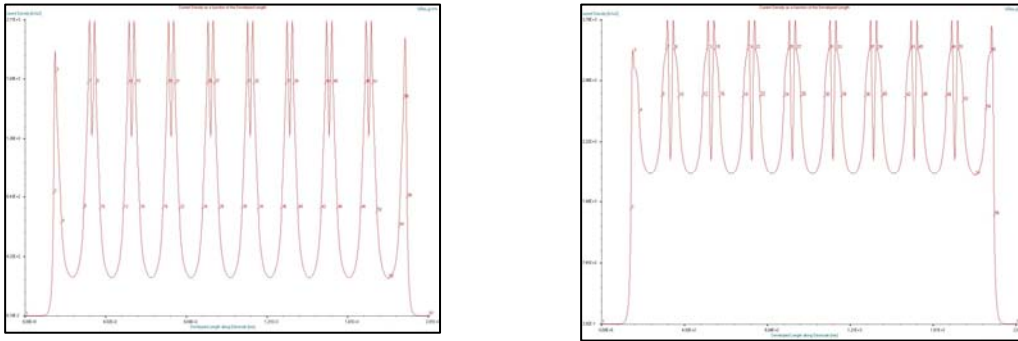


Fig. 5.4: Calculated current distribution without (left) and with (right) radial rods in order to increase the current density at the equator region

The transfer of EP technology to industry has been started. Contracts to industry were placed for the installation of 9-cell EP facilities (ACCEL, HENKEL). These installations follow the experience of the prototype operation at DESY. The first operation is expected for early 2008.

5.3 Automated EP

At INFN laboratory an automated EP system was developed and tested with single cell Nb resonators (see CARE-Report-07-010-SRF). A collaborative effort of INFN Legnaro and DESY has been started to adopt the necessary electronics and software to the DESY 9-cell EP facility. It is expected to turn the DESY EP facility into automated operation early 2008.

5.4 Dry ice cleaning.

A set-up for the horizontal cleaning of single- to three- cell cavities is in successful operation. The present parameter set of DIC gives reproducible gradients of 35 MV/m in single-cell cavities with no or low field emission loading (see Fig. 5.5)

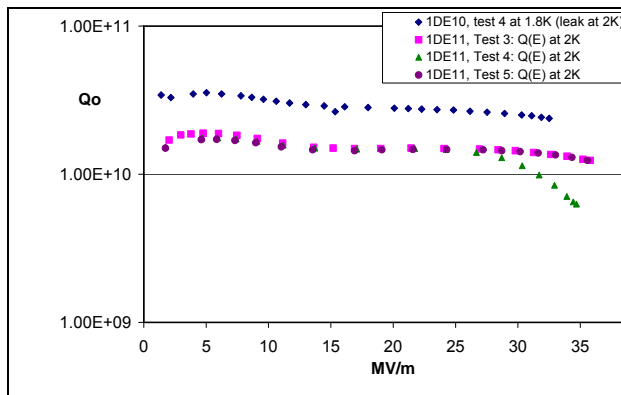


Figure 5.5: Q(E)-performance of the latest 4 DIC cleaned cavity tests

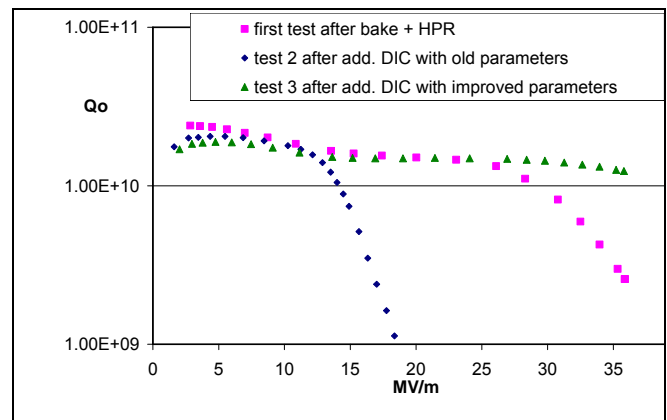


Figure 5.6: Q(E)-performance of one single cell cavity after HPR (test 1, pink), DIC with old parameters (test 2, blue) and DIC with improved parameters (test 3, green)

There are examples where dry ice cleaning (with the modified cleaning parameters) exceed the cavity performance gained after high pressure water cleaning (see fig. 5.6).

In order to provide low dark currents in the gun cavity of the photo injector of FLASH and for the future European XFEL, a dedicated dry ice cleaning set-up (Figure 5.7) was constructed, commissioned and recently started up. Compared to the previously applied cleaning using HPR, the risk of an objectionable oxidation of the sensitive rf surface is minimized.

Remarkable is the new nozzle system with a 110° degree rotatable nozzle (Figure 5.8). This design is necessary in order to assure a complete and effective cleaning of the rf gun geometry, i.e. the surface close to the cathode and the first cell of reduced length. In order to avoid any particulate recontamination created by the motion of the nozzle, the nozzle system is exhausted.

The first gun cavity has been cleaned recently, and the cavity test is under preparation.

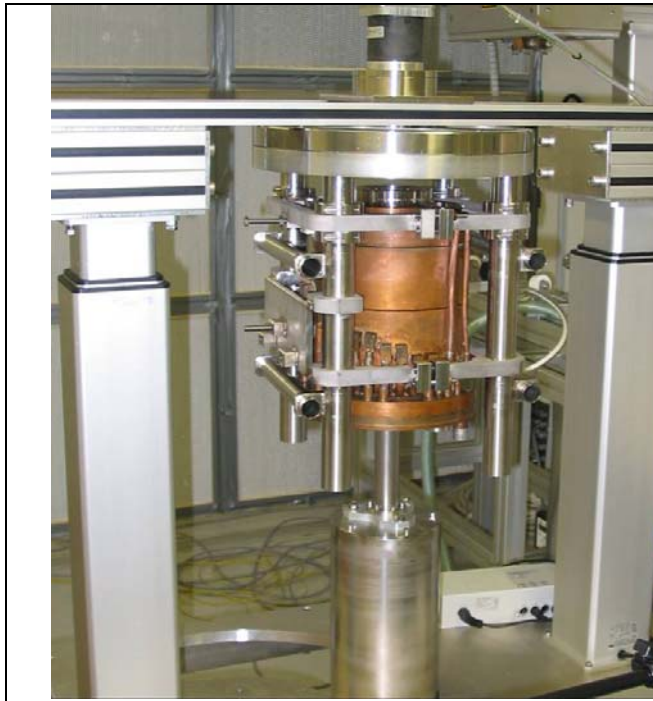


Figure 5.7: Vertical cleaning set-up for copper rf gun cavities

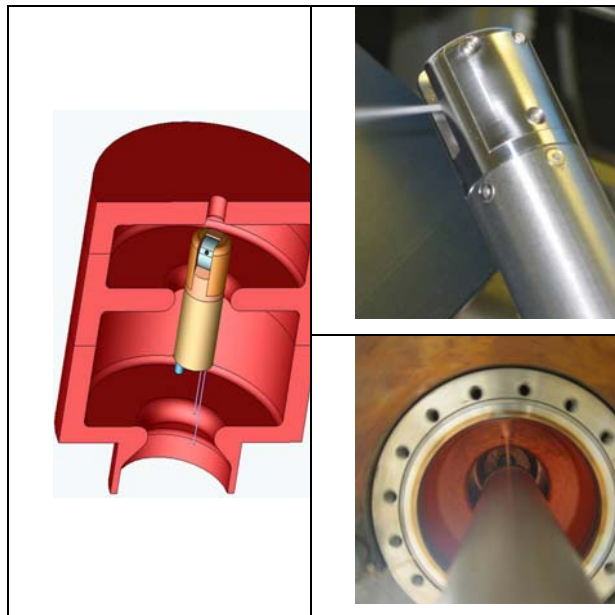


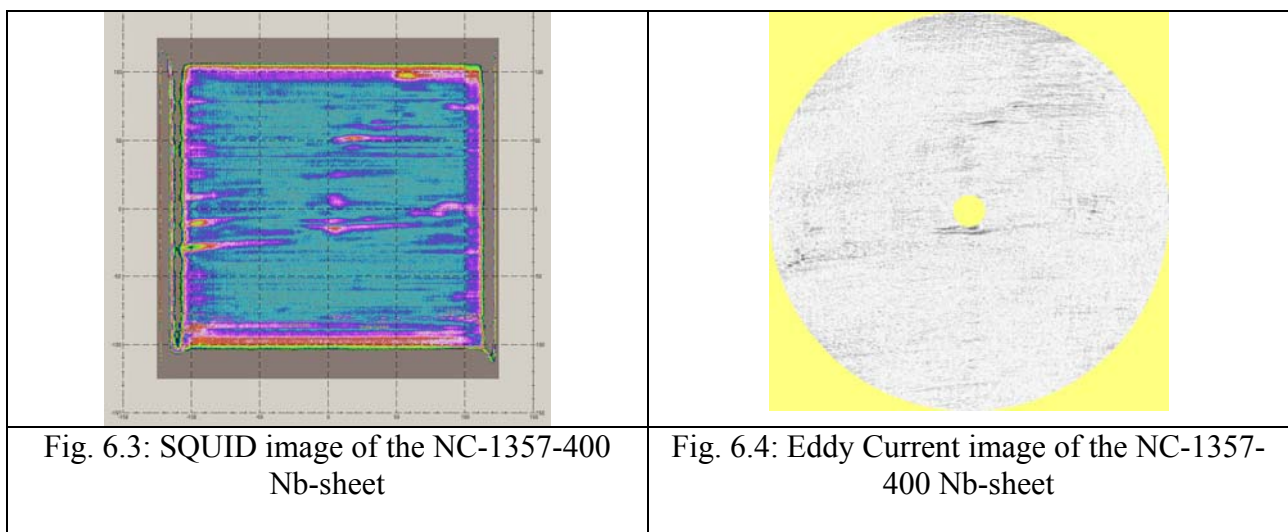
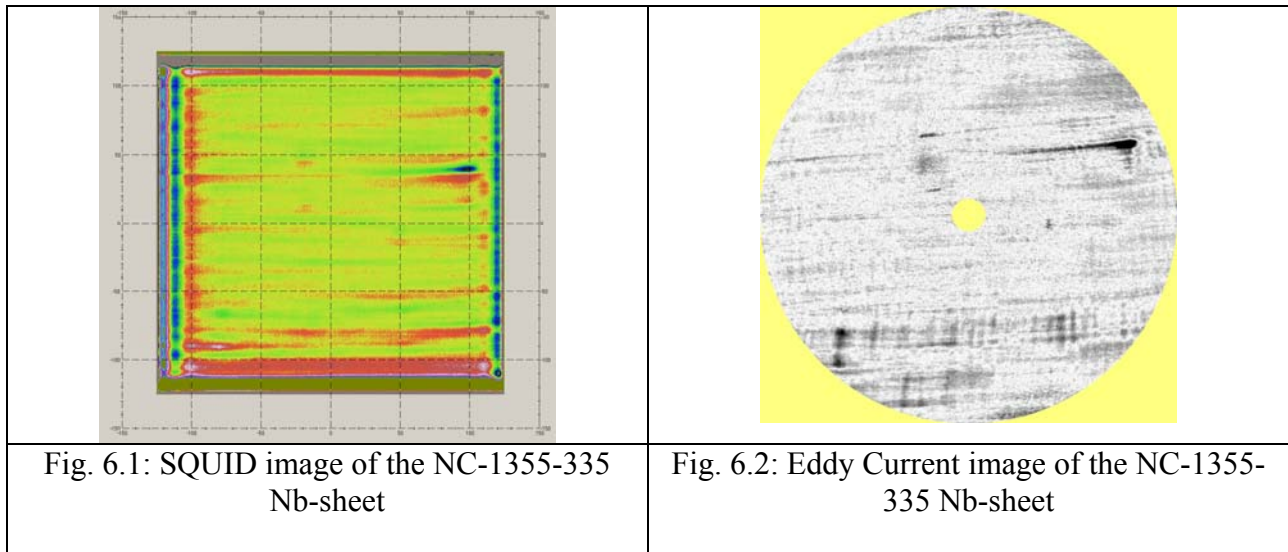
Figure 5.8: 3D-model of gun cavity with rotatable nozzle (left); rotatable nozzle (upper right); bottom-up view of the cleaning of the gun cavity (lower right)

WP 6 Material Analysis (MA)

Task 6.1 SQUID scanning results

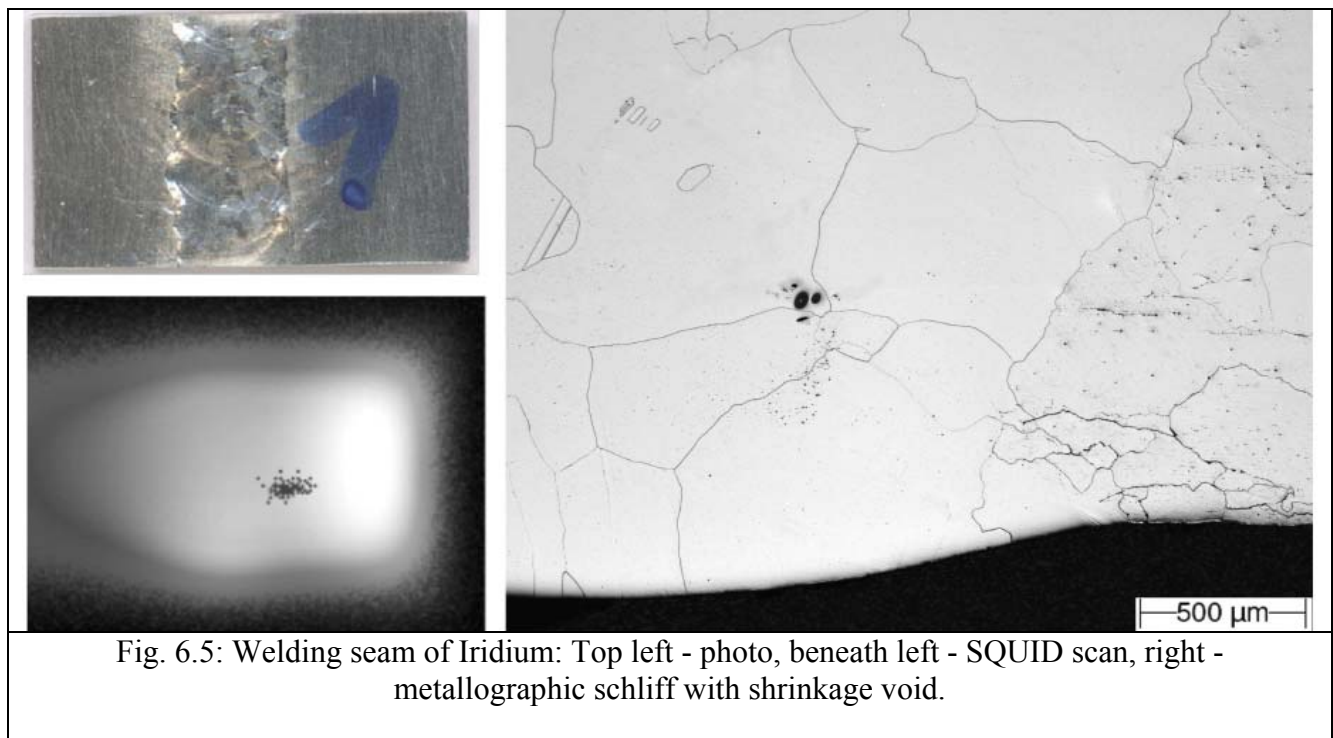
Further improvement of the SQUID scanner has been further improved and a special software tool has been developed which allows minimizing the noise signals caused by vibration etc. Excitation frequency was significantly increased up to 80 kHz.

21 niobium sheets of the Fa. Tokyo Denkai has been scanned with WSK SQUID scanner. In addition another 20 sheets from Plansee company have been scanned, too. SQUID scanning results have been compared with Eddy Current scanning results get for the same sheets earlier. The sensitivity of the SQUID apparatus is at least on the same level as of the EDDY current apparatus. Two examples of the comparison can be seen in the figures 6.1-6.4.



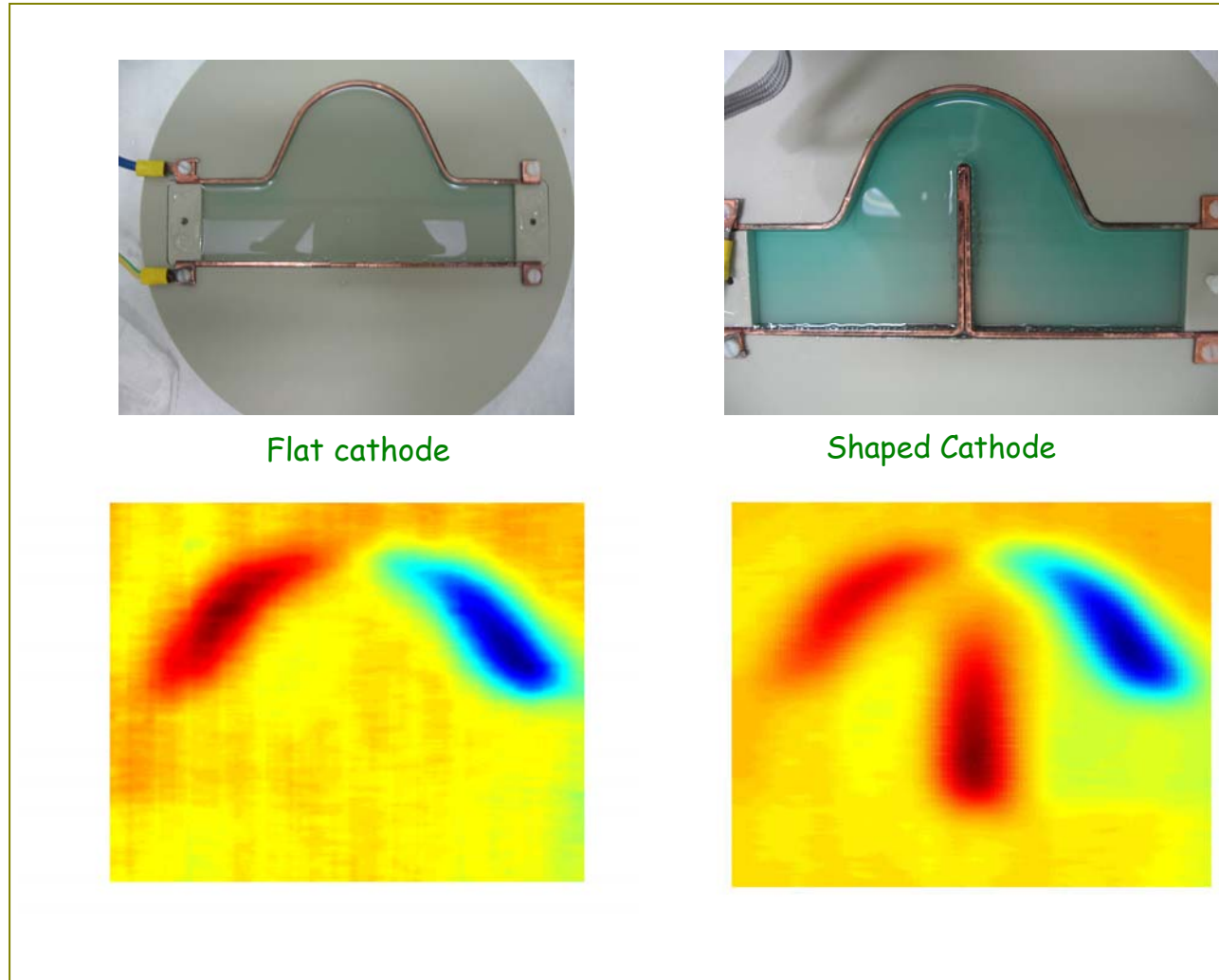
It can be seen that for the sheet NC-1357-400 the SQUID sensor makes existing flaws even more visible than by the eddy current method

Another evidence of the high sensitivity of SQUID apparatus have been obtained at WSK on the irridium welding seam. Shrinkage voids smaller as 50 μm have ben detected by SQUID and have been clearly proven by metallographic investigation (see Fig. 6.5)

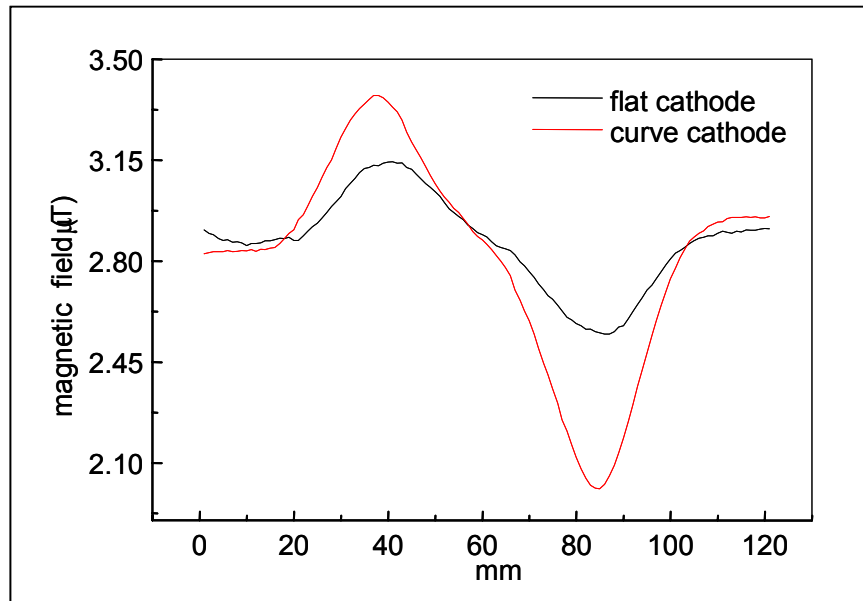


Task 6.2 Flux gate magnetometry

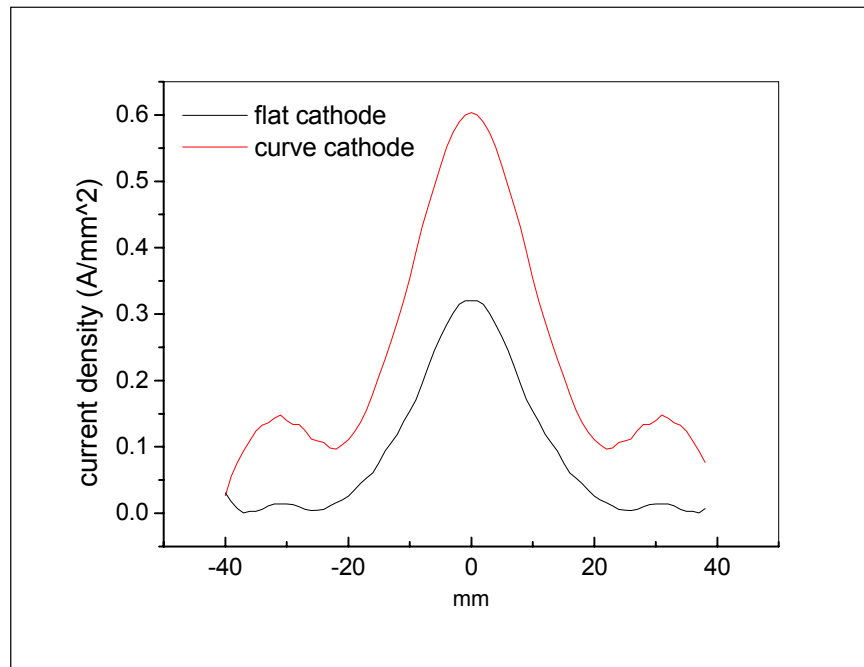
After having compared flux gate sensors with GDR, we have seen that both GDR and flux gates, whenever applied to the cavity electropolishing, show the same result, i.e. a shaped cathode works definitely better than a flat electrode. The cavity section shows that the viscous layer is more uniformly distributed in the case of shaped electrode, while there is a difference in the cell magnetic map, but this is quantitatively an information difficult to interpret.



In the next figure the maximum intensity of magnetic field along the cavity internal wall is mapped along the cavity axis, and from this picture it is already understandable that the magnetic field at the equator is higher for the shaped cathode case.



Therefore, we used the inversion of magnetic field maps, in order to get the current distribution along the cavity profile for the two different cathodes. The result in the figure below, where the current distribution is plotted versus the cathode length, showing that the effect at the equator is almost doubled.



In synthesis, the experiment definitely proves that the EP cathode should not be a simple tube but a shaped electrode. It is obvious that the insertion of such a cathode inside a cavity could be difficult, however an umbrella type cathode would give the advantage of a uniform thickness removal during EP.

Task 6.3: DC field emission scanning

Here we report about the effectiveness of dry ice cleaning (DIC) to suppress the enhanced field emission (FE) from crystalline Nb samples of very good surface quality. Three large grain Nb samples with 30 μm BCP +HPR, which had shown the onset of FE at high field of 150 MV/m, were dry ice cleaned at DESY and were measured again with a field emission scanning microscope. A new series of four large grain Nb samples, with increased BCP layer thickness of 100 μm was also prepared at DESY for systematic FE measurements on crystalline Nb samples. The surface treatments and measurement details of the samples are listed in the table below.

Sample	Surface treatment/ Production method	Intermediate measurements	Final treatment	Measurement, Analysis
SCNb1	30 μm BCP + HPR	FE measurements, SEM, EDX	Dry Ice Cleaning	FE measurements, SEM, EDX
SCNb2				
CryNb1		FE measurements		
ScNb3	100 μm BCP + HPR	FE measurements, SEM, EDX	--	--
CryNb3				

The main results of this work can be summarized as follows:

I. Dry Ice Cleaned large grain Nb samples (30 μm BCP):

- The onset of FE for single crystal Nb samples in the regulated V-scans for 2 nA current was observed at 200 MV/m, showing a positive shift from 150 MV/m (before DIC) for the same scanned area.
 - FE particulates down to 400 nm were observed to be removed by DIC and the effect of DIC on surface irregularities was observed for the first time. SEM images in Fig.6.6 and 6.7 show the removal of the delamination and partial smoothing of sharp scratch-edge-features by DIC. The scratch in Fig. 6.6 showed field emission at 60 MV/m before DIC, while no emission up to 150 MV/m after DIC was observed.
- ⇒ It proves that DIC is capable to efficiently suppress FE caused by particulates as well as surface irregularities like scratches.

II. Large grain Nb samples (100 μm BCP):

- First evidence was found for the higher onset field with the increased BCP treatment. The onset of FE for single crystal Nb was observed at 200 MV/m for 100 μm BCP and 150 MV/m for 30 μm BCP. The emitter density at 250MV/m is 9 and 16 /cm² for ScNb3 and CryNb3 samples.
- Locally measured emitters showed stable FN behavior after current processing. Reduced local field enhancement factors between 20 to 85 and S parameters in the range of 10⁻¹ to 10⁻⁸ μm^2 were observed, which are typical for particulates and surface irregularities.

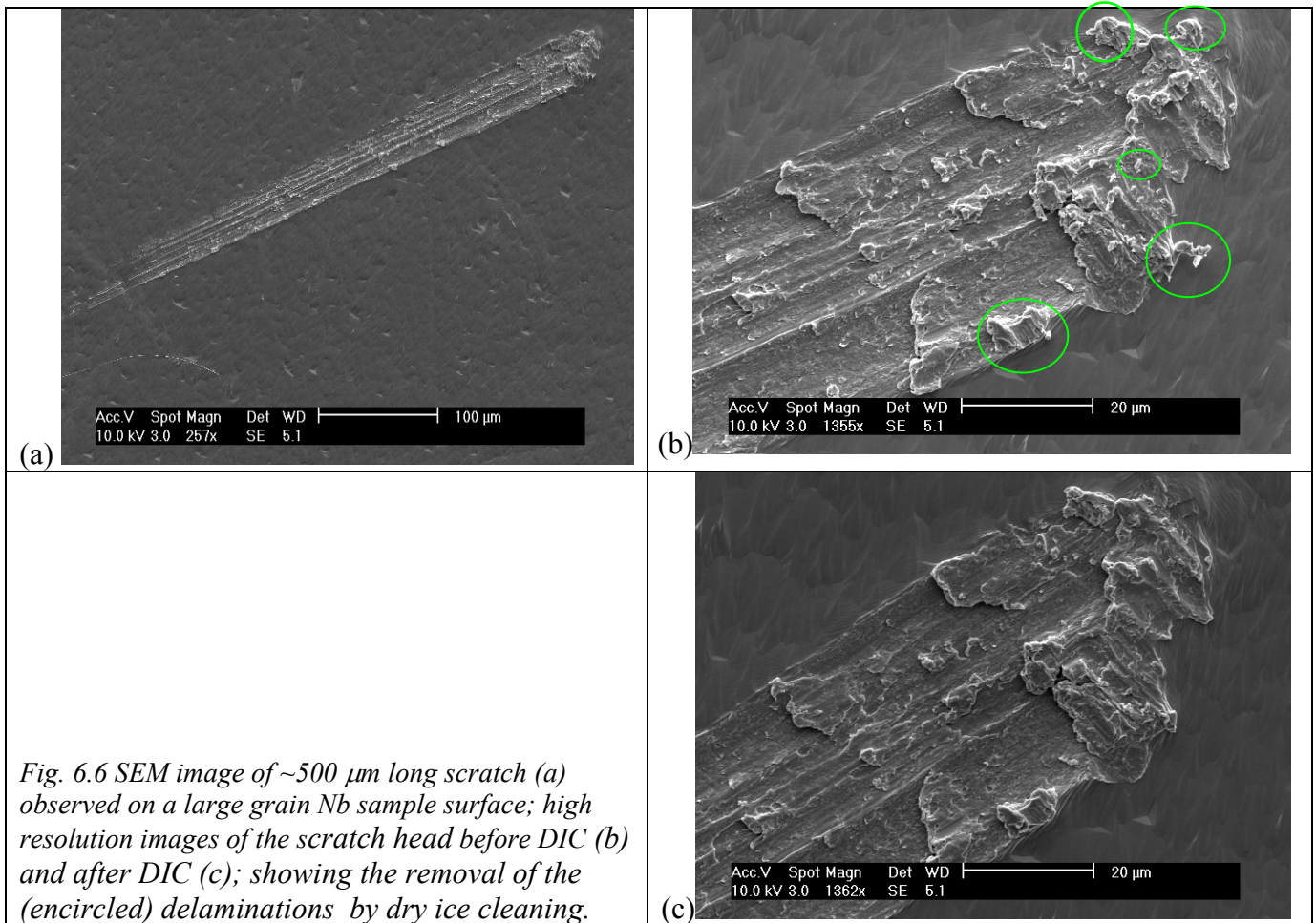


Fig. 6.6 SEM image of ~500 μm long scratch (a) observed on a large grain Nb sample surface; high resolution images of the scratch head before DIC (b) and after DIC (c); showing the removal of the (encircled) delaminations by dry ice cleaning.

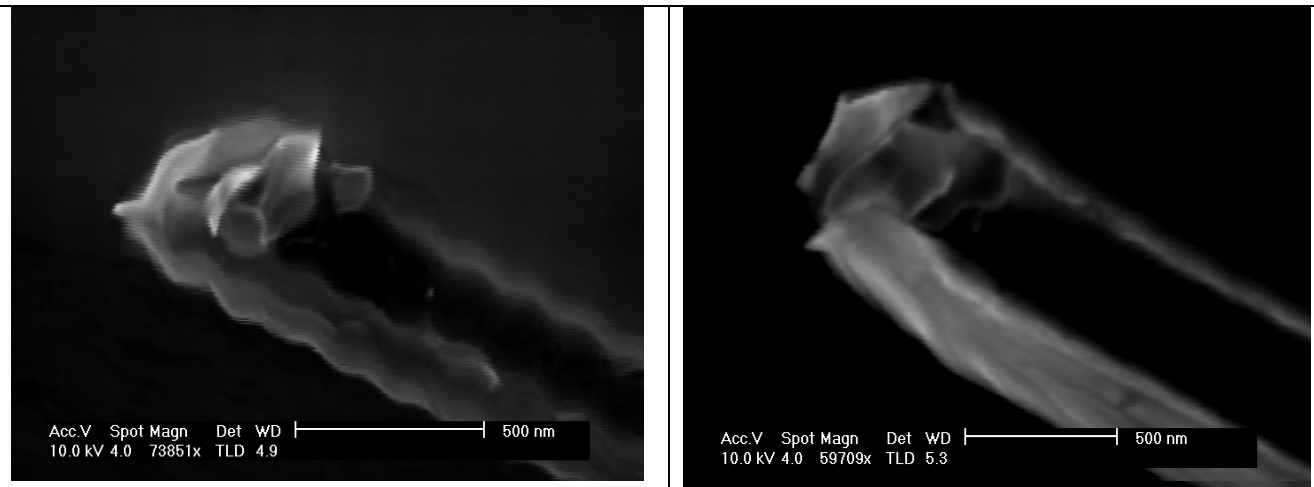


Fig. 6.7 High resolution SEM images of a scratch head before (left) and after (right) DIC, showing partial smoothing of the scratch –edge-features.

To complete the systematic study, detailed analysis are ongoing on the rest of the measurements performed over 100 μm BCP treated large grain Nb samples.

WP 7 Couplers (COUP)

Task 7.1 : New coupler prototypes :**TTF-V :**

The RF inspection of the two new TTF V couplers detected that the optimum transmission frequency was shifted by 20 MHz from 1.3GHz to 1.32 MHz. This is most likely due to mechanical fabrication errors or a deviation of the dielectric constant of the RF window material. In order to proceed with the high power high test of the couplers a standard microwave technique was applied: additional mechanical changes are introduced to RF compensate the original mistake. This was possible by changing every coupler antenna penetration in the waveguide test box from 33.75 mm to 27.75 mm. In addition some spacers were added between each cold part flange and the respective waveguide test box flange. Using this solution, we found that the two TTF-V coupler pairs now have a perfect match at the operating frequency of 1.3 GHz (minimum reflection coefficients less than -40 dB, see figure 7.1).

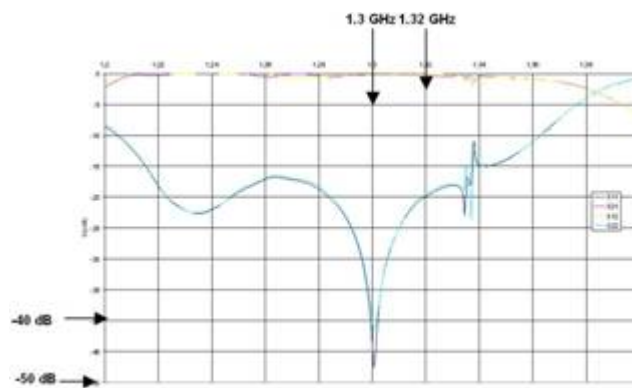


Figure 7.1: Optimum transmission (i.e. minimum reflection) of the first TTF V couplers at 1.3 GHz after correction of the mechanical tolerances by RF compensation technique.

High power RF tests of the TTF-V couplers are planned in December 2007.

TW60 :

After fabrication the coupler pair was cleaned with the TTF-III couplers cleaning procedure. The TW60 pair was also baked under vacuum in the class 10 room oven at 150°C. After assembly the couplers were baked in-situ at 130°C. The design of these couplers offers large pumping ports for better pumping performances, but unfortunately we had to use the same pumping arrangement than for the TTF-III processing.

Low power level RF measurements illustrated a minimum reflection at 1.3 GHz of less than -32 dB. The RF matching was possible thanks to the position adjustments of the RF stub located in the warm waveguide part of the coupler. No significant RF leaks were detected through the RF choke used to screen the bias system from the RF power.

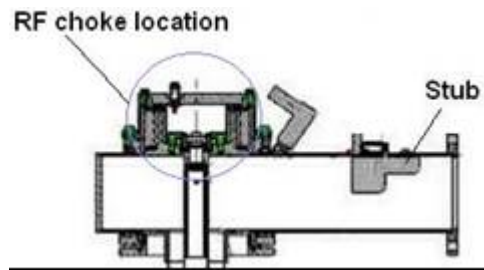


Figure 7.2: Warm waveguide part of the TW60 coupler.

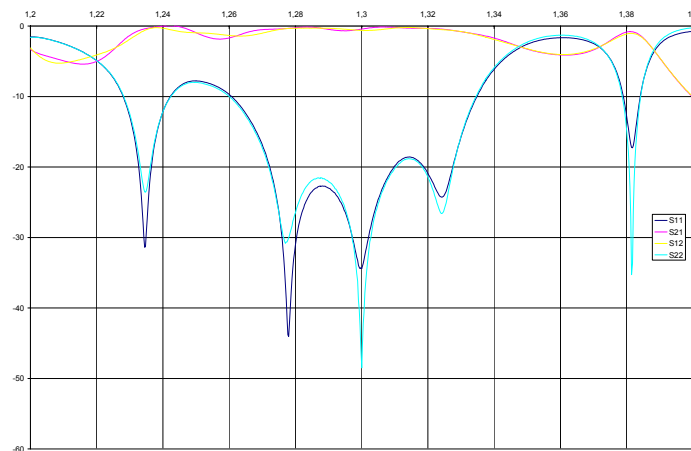


Figure 7.3: Comparison of calculated and measured minimum reflection data of the TW60 coupler pair assembly at 1.3 GHz. Upper curve is the measured transmission power.

A RF processing of the pair of couplers has started using 20 μs pulses. The processing seemed to be long and many vacuum and current interlocks took place. The most limiting factor was the e-currents interlocks for any exceed of 5 mA. We also noticed that the e-current enhancements take place at a precise power levels and decrease drastically at some others. A progressive decrease of e-current levels was possible at all processed power levels.

As there is some differences between the shape of the TW60 pick-ups and those of TTF-III, we can't make an exhaustive comparison between their relative e-current issues at this time.

The maximum power reached was 660 kW. The conditioning was stopped for the annual maintenance of the modulator cooling water system. Many ramps of power was made before this stop. They showed that, after this processing period, we can increase power easily to 660 kW

without having any interlocks. Besides, vacuum steel relatively low below this RF power level.

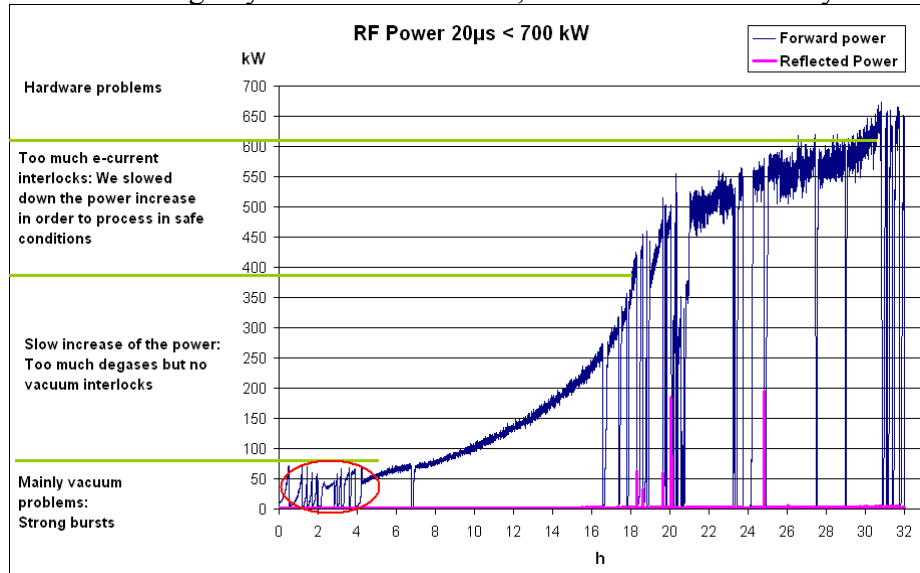


Figure. 7.4: Conditioning of TW60: Processing was interrupted due to hardware problems

Task 7.2 : Titanium nitride coating bench for the coupler ceramic windows

Concerning the task 7.2, a new recruit in post-doctoral position has joined the team since April 2007 to work on TiN sputtering in coupler ceramic windows.

In order to prepare the reception and the installation of coating bench in LAL, a visit was made at the beginning of May to our collaborator at Ferrara Ricerche (Italy). This allowed us to follow the advance of machine assembly, to note works to undertaken and to discuss the next steps to be carried out.

During this visit, we have noted that the machine assembly is still in progress (see photos).



It was also the opportunity to discuss the best way to move sample holder to obtain the best deposit accordingly to the specifications.

The fitting out of the local where sputtering bench will be installed is already started. Partitions and ceiling installation, electrical and computer work as well as plumbing and ground painting are programmed. The end of this works is planned before the end of July, just on time to receive the machine.

As mentioned in the contract, before the reception of coating machine, the person who will work on it will spend one week in Italy in order to make first experimental tests and checks. Once that the process is validated the machine will be transferred to LAL. Here an expert from Ferrara Ricerche will assist to the final in situ test of the coating bench that will take to the acceptance or refuse of the machine.

Task 7.3 : Conditioning studies of TTF-III couplers:

We still maintain a conditioning time between 19 h and 24 h. The last result obtained in 05 Mai 2007 was about 23 h of conditioning time. Future test aims to reach better performances.

WP 8 Tuners (TUN)

8.1. UMI Tuner

The cold test of the coaxial piezo/blade tuner (UMI Tuner) was prepared at DESY and for the horizontal test facility CHECHIA. The TTF cavity Z86 has been chosen to be installed into a modified helium tank, where a central bellow allows for coaxial tuning. In figure 8.1 the two ends of Z86 9 cell cavity are shown after EB welding of the rings at Lufthansa machine shop.



Figure 8. 1: Z86 cavity after the rings EBW at Lufthansa facility

The cavity integrated in the modified helium tank, after TIG welding at DESY, is shown in figure 8.2.



Figure8. 2: Cavity integrated in the modified helium tank in Halle III at DESY

The placing of the coaxial tuner assembly and the cavity warm tuning operation will take place between August and September, followed by the preparation for CHECHIA.

Meanwhile, a new design of the blade tuner has been developed in order to optimize the total cost of the apparatus and improve the performance. The starting point of this final design is the existing blade tuner that proved to fulfill the slow tuner requirements. For this purpose two alternative prototypes have been recently designed and built. They mainly differ in the used materials (titanium or stainless steel). They have been optimized to minimize material and construction cost, while fulfilling the reviewed performance required for the high gradient cavity operation up to 35 MV/m (or even higher). The new prototypes' main features are:

- **Lightness:** The redesign of rings allowed an important weight reduction (about 40%) maintaining the full symmetry with collinear blades.
- **Highest tuning range:** The different blade geometry improves the slow tuning capabilities to more than 1.5 mm at the cavity level.
- **New Driving Mechanism:** The new driving mechanism is simpler, cheaper and more compact, simplifying the installation of an external magnetic shield.
- **Compliance with future steel tanks:** The tuner can be built both with titanium or stainless steel rings. The use of a high strength alloy for blades allows to exploit the full tuning capabilities without plastic strains.
- **Low cost:** The new geometry and mechanism lead to an important reduction of costs.

Figure 8.3 shows the the new tuner installed on the current modified TTF/FLASH helium tank.

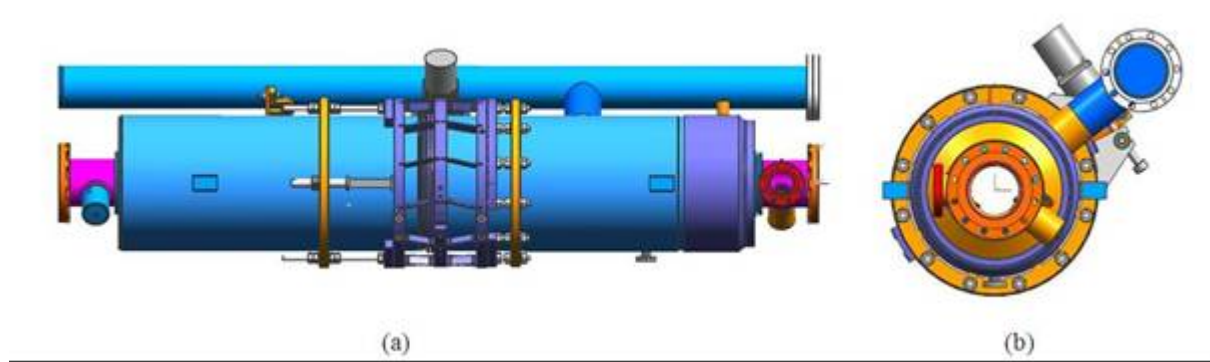


Figure 8. 3: the new tuner installed on the TTF helium tank. Lateral (a) and frontal (b) view.

The new tuner, together with the revised driving system, mounted on a single cell test apparatus, is shown in figure 8.4.



Figure 8. 4: the optimized coaxial tuner for ILC.

Together with DESY and TUL we are working for the compensation of Lorentz Force Detuning (LFD) for FLASH cavities. A algorithm for optimum LFD compensation is developed and implemented into the FPGA based boards, such as SIMCON 3.1 LLRF boards. In figure 8.5 an example is shown, where one can see the compensation with pulsed piezoelectric ceramics of the whole detuning of cavity 3 in Module 6 at MTS, operated at 35 MV/m.

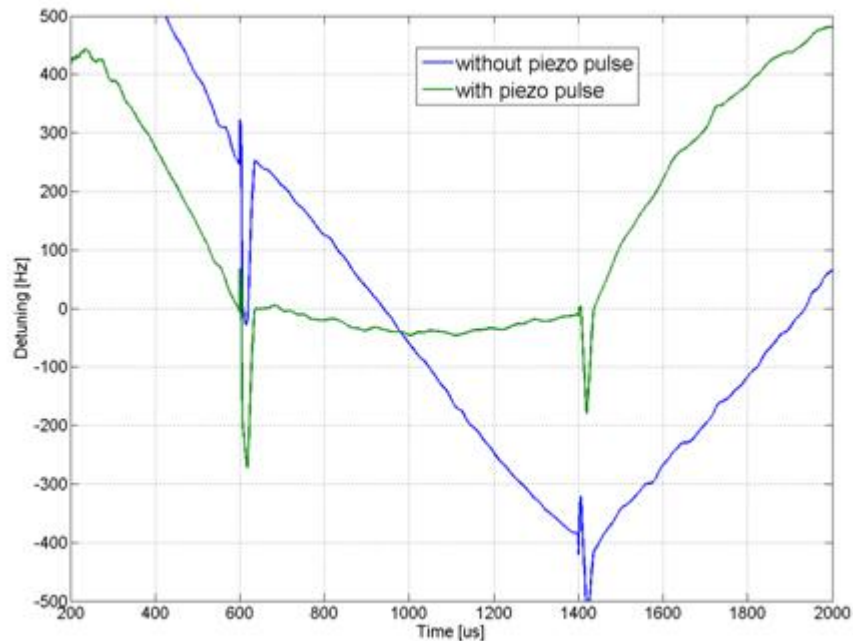


Figure 8. 5: detuning of cavity 3 in Module 6 at MTS, operated at 35 MV/m.

8.2. Magnetostrictive tuner

The prototype of magnetostrictive tuner is ready for test with the cavity. The control system as well as the driver have been completed. Due to the movement of the CRYHOLAB, the experiment with magnetostrictive tuner is postponed. According to the recently updated schedule, the test will be done before end of the year.

The control algorithm has been developed for both piezostack and magnetostrictive operation. The worked out algorithms were implemented in the FPGA-based control system. The SIMCON board is used, which allows to perform parallel, deeply pipelined calculations (see figure 8.6). The new approach allows integrating the algorithm dedicated for cavity shape control with the LLRF system used for vector sum control.

The new algorithm for on-line detuning calculation which is based on the electromechanical model of the cavity is presented.

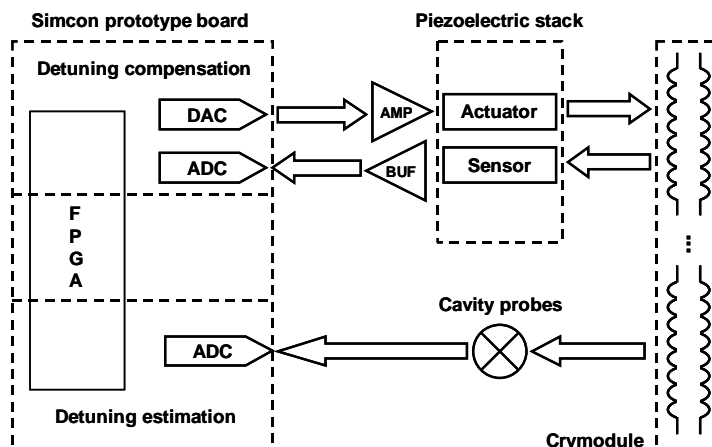


Figure 8. 6: Block diagram of control system

The system was tested with Module Test Stand (MTS) at DESY with the high gradient cavities (up to 37 MV/m). The results are presented in figure 8.7.

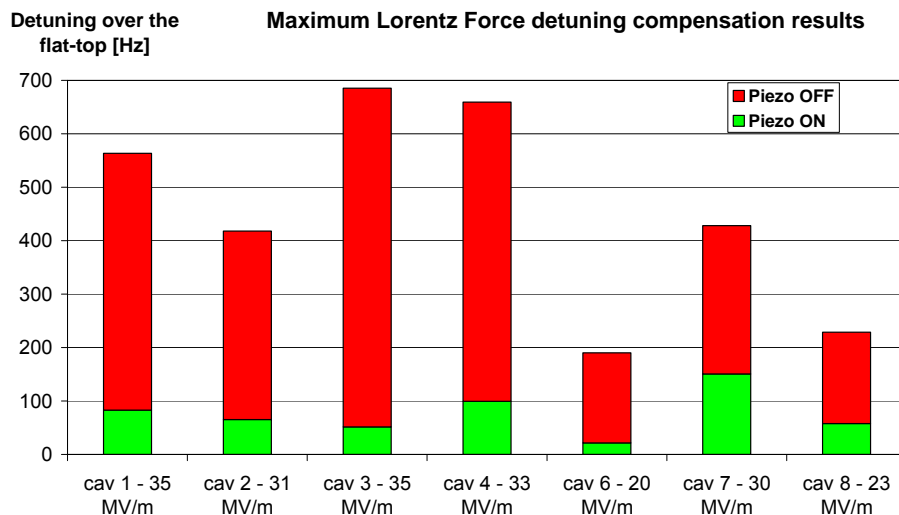


Figure 8. 7: The results of detuning compensation

The best results of active Lorentz force compensation was observed for cavities 1, 3 and 4 which were detuned at gradients of 35 MV/m. The detuning over the flat top region for cavity 3 was decreased from around 700 Hz down to 50 Hz. The output signal for cavity 5 was too small to receive appreciable results.

For the digital control system test purpose, a simple cavity simulator has been developed. The raw data sampled from the operational system are taken from DOOCS servers. The samples are stored in internal BRAM memory blocks of Virtex II Pro FPGA. The system is driven by a trigger signal with flexible range (2-10 Hz) repetition rate, as in the RF pulse operating mode. A strobe signal with 1 μ s period time is also added. The simulation data can be easily changed using a C++ control application running on an embedded Sparc computer. The system also contains a MUX, which allows selecting the results from various processing blocks. The results can be easily analyzed using Matlab environment.

The results were published in the PAC07 conference. The acquired results connected with static force measurement was published in the MST-IOP Journal.

8.3. CEA Tuner

The new CEA tuner has been completed, mounted and tested in CRYHOLAB.

8.4. IN2P3 activities

The final report, which is a deliverable for WP8 was submitted. A CARE note dedicated to the radiation hardness of elements was also published. Both documents summarize the previously performed experiments detail. The results were also presented on MIXDES conference and in the MST-IOP Journal.

WP 9 Low Level RF (LLRF)

9.1 Operability and technical performance

9.1.1 Transient detector

During 2007 the activities were focused on development of the cost-effective version of transient detection system and on improvements of the measurement accuracy.

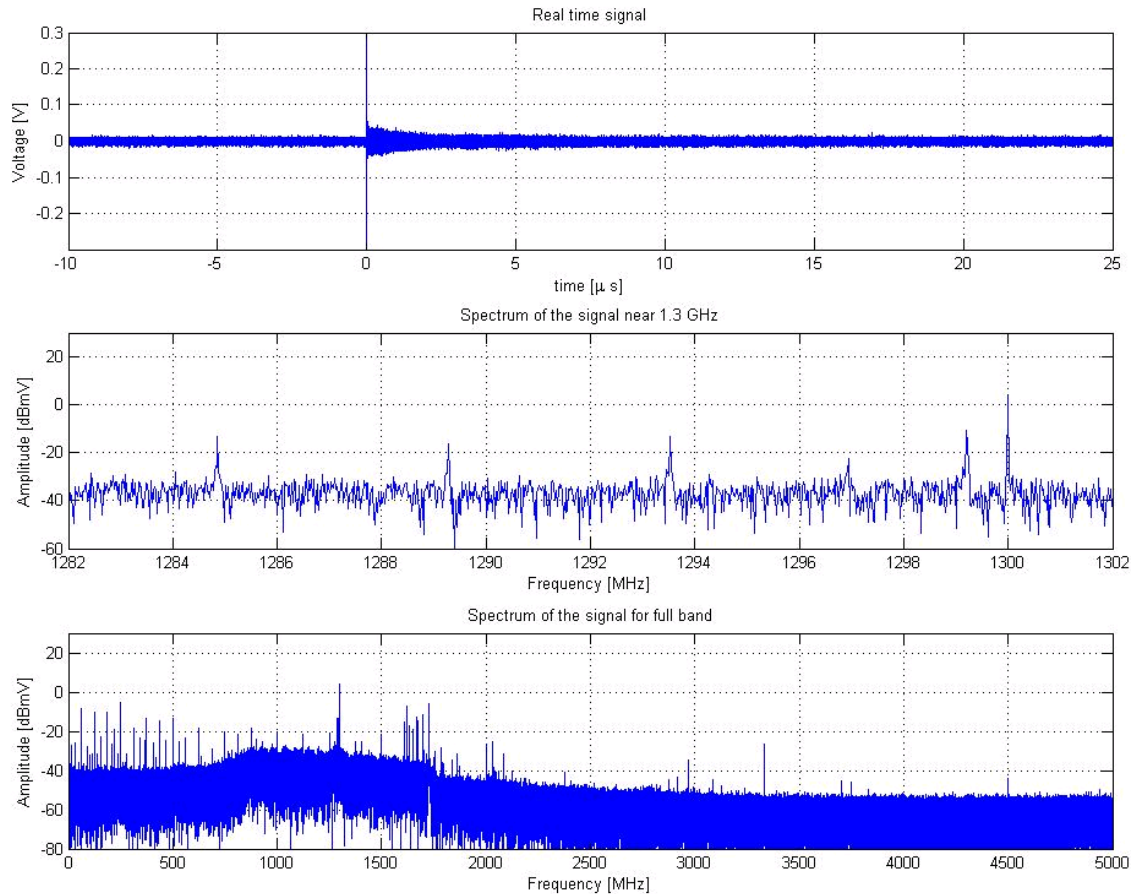


Figure 9.1. The transients induced by single bunch

Many measurements have been made to investigate the influence of signals coming from excitation of the other passband and higher order modes. The single bunch induces transients (Figure 9.1 – upper part) not only at the base resonant frequencies of cavity (1300.091 MHz) but also at others passband frequencies (1299.260 MHz, 1296.861 MHz, 1293.345 MHz, 1289.022 MHz, 1284.409 MHz – Figure 9.1 – middle and bottom parts) and even higher order modes. The transient detection system measures the sum of transients at different resonant frequencies of cavity and therefore the measurement accuracy is limited. The already demonstrated performance of the transient detection system is absolute accuracy of few degrees in phase. The new method which is currently evaluated is based on the measurements of higher order mode excited by electron beam with respect to the RF generated by klystron. This method gives the relative beam phase and requires calibration by absolute beam phase measurement.

9.1.2 LLRF Automation

Automation:

During 2007 the activities were focused on improvements of general framework for designing and development of automation software for the FLASH (Free-Electron Laser in Hamburg). The ultimate goal of the framework is to systematize the way of automation software development and to improve its dependability. The principal results of the latest work concerning automation belong to three different areas.

- The methodology of designing automation software for such installations as the FLASH.
- The domain specific languages supporting practical specification and implementation of the automation software.
- Implementation of general expert system infrastructure.

The most significant achievements are enumerated below:

1. The methodology of automation design.

- Utilization of UML (Unified Modelling Language) diagrams for specification preparation, which facilitates cooperation with the system experts
- Implementation of the tool facilitating perceptual evaluation of the specification for the planner
- Implementation of several algorithms for verification of syntactical correctness of the specifications
- Utilization of constraint solvers for verification of certain aspects of semantical correctness of the specification
- Integration of formal verification tools into the process of automation software design
- Implementation of the testing environment which facilitates the automation software introduction.

2. The domain specific language for automation design and implementation.

- The specification language allows to design the automation scheme using domain specific nomenclature which is understood by the system experts and the operators, namely: operation modes, activities, exceptions, to name a few.
- The specification language is also an implementation language, therefore designed automation scheme can immediately be put into practice.
- The language offers expandability in automation design. Adding a new task to be automated does not involve redesigning of already specified tasks.

3. The general expert system infrastructure.

- Unlike the DOOCS (Distributed Object Oriented Control System) state machines or the EPICS (Experimental Physics and Industrial Control System) sequencers the planner is equipped with state estimator keeping the active state of the finite state model of the plant in sync with its physical condition.
- Improvement of dependability of the automation software by formal verification of cooperation protocol assuring correct causal behaviour of automation software modules.
- Elaboration of method for resolution of conflicts among mutually occurring exceptions.

All the methods and tools mentioned above have been tested in proof-of concept automation for the RF-station (Radio Frequency) for the FLASH.

Linearization of the high power chain of the RF control system.

The method of linearization of the high power chain of the RF system based on the pre distortion was implemented in LLRF (Low Level Radio Frequency) control system field controller called SIMCON 3.1 (**S**imulator-**C**ontroller) based on FPGA (Field Programmable Gate Array) chip.

The operator panel was created as a part of software control system DOOCS (widely used in the FLASH operation). Mentioned graphical user interface is used for characterisation and linearization of the high power components.

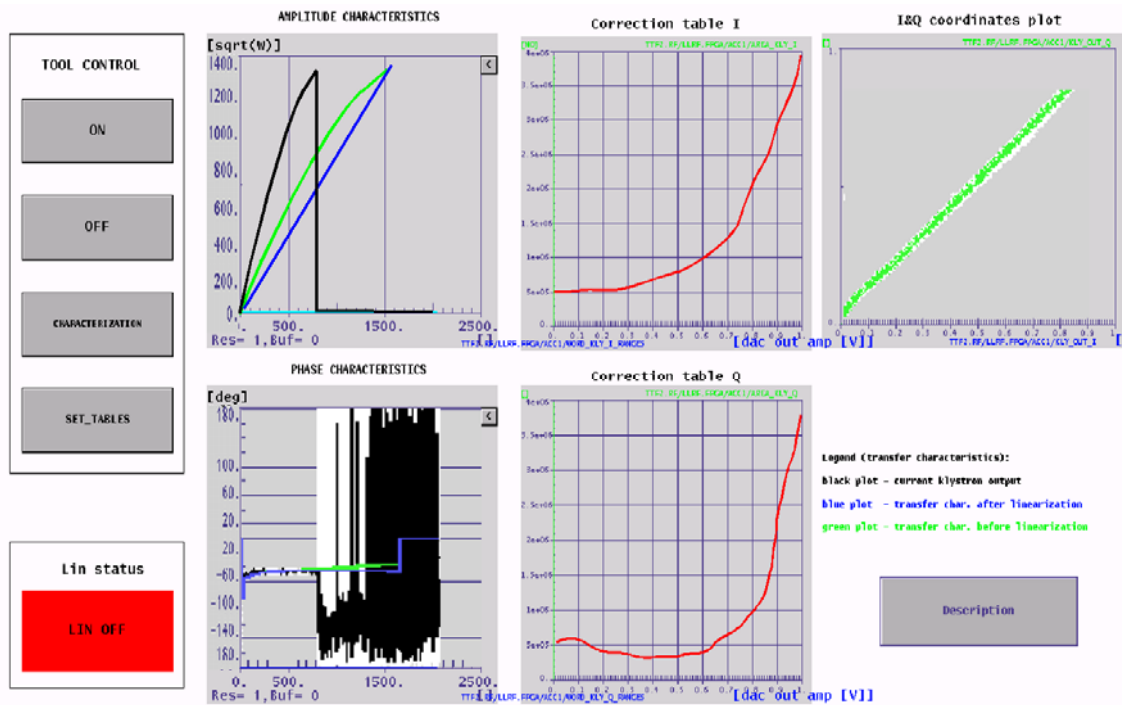


Figure 9.2. Characterization and linearization tool management panels for the klystron 2. Prepared and evaluated tool for the RF system amplifiers chain characterization and linearization allowed for the transfer characteristics (amplitude and phase) linearity improvement. Implementation of the presented tool in the ACC1 (**A**ccelerating Module) LLRF controller give an opportunity for comprehensive study of the amplifiers amplitude and phase deviation's in case of the amplifier chain components exchange or system work conditions change (for instance various high voltage level of klystron).

9.1.3 Control Optimization

During 2007 the novel firmware implementation was still developing to investigate the optimal control methods for LLRF system. The control algorithm based on the system identification is the proposal verified by the experimental results. It has been introduced in the ACC1 module of the FLASH. Moreover, the MTS (Module Test Stand) setup in DESY has been remotely controlled from the WUT-ISE laboratory in Warsaw. The general idea realized as Multi-Cavity Complex controller (MCC) is presented below (Figure 9.3).

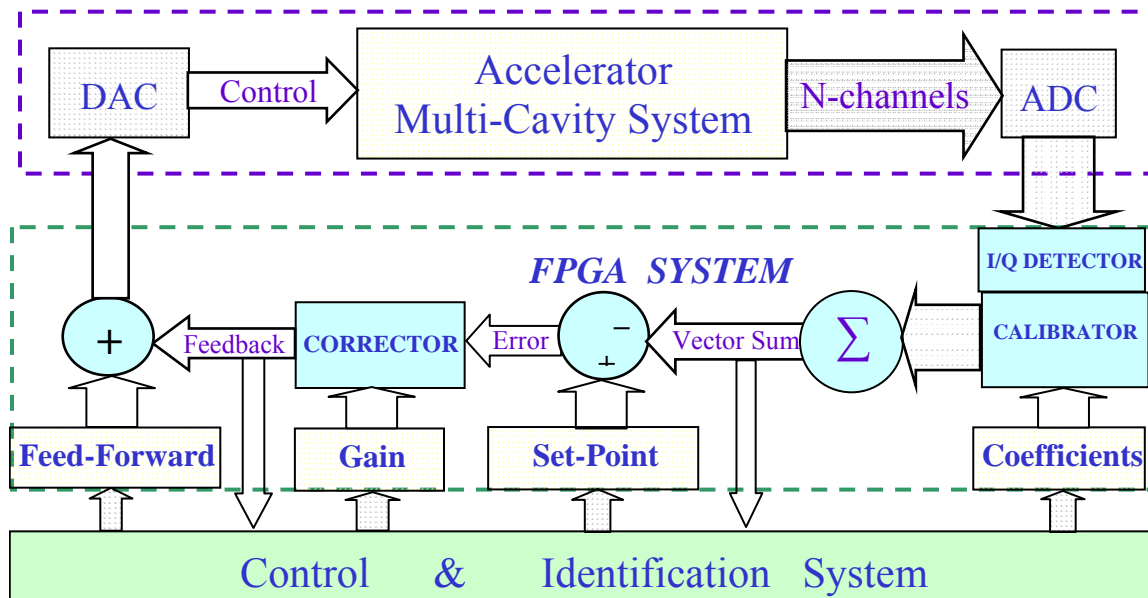


Figure 9.3 Block diagram of Multi-Cavity Complex controller for LLRF system

The required cavity performance is to drive in the resonance during filling and to stabilize the field for the flattop range. The multi channel auto-calibration is considered for a vector sum control. The cavities module is driven in a feedback mode supported by feed-forward to fulfill desired operation condition for the vector sum. The FPGA based controller executes procedure according to the prearranged control tables: Feed-Forward, Set-Point and Corrector unit. Nonlinearities and deterministic disturbances are compensated by feed-forward table for the open loop operation (Figure 9.4). The closed loop correction (tuning) for the feed-back mode is performed by a complex gain of the Corrector table. It also includes the klystron linearization. The loop gain value 300 has been achieved for the vector sum control of ACC1 at FLASH. The adaptive control algorithm is applied for feed-forward and feedback modes according to the recognized process. The presented method is useful for the repetitive, deterministic condition what has been verified experimentally. Achieved field stabilization: amplitude relative accuracy $\sim 10^{-4}$, phase accuracy $\sim 2 \cdot 10^{-4}$ rad.

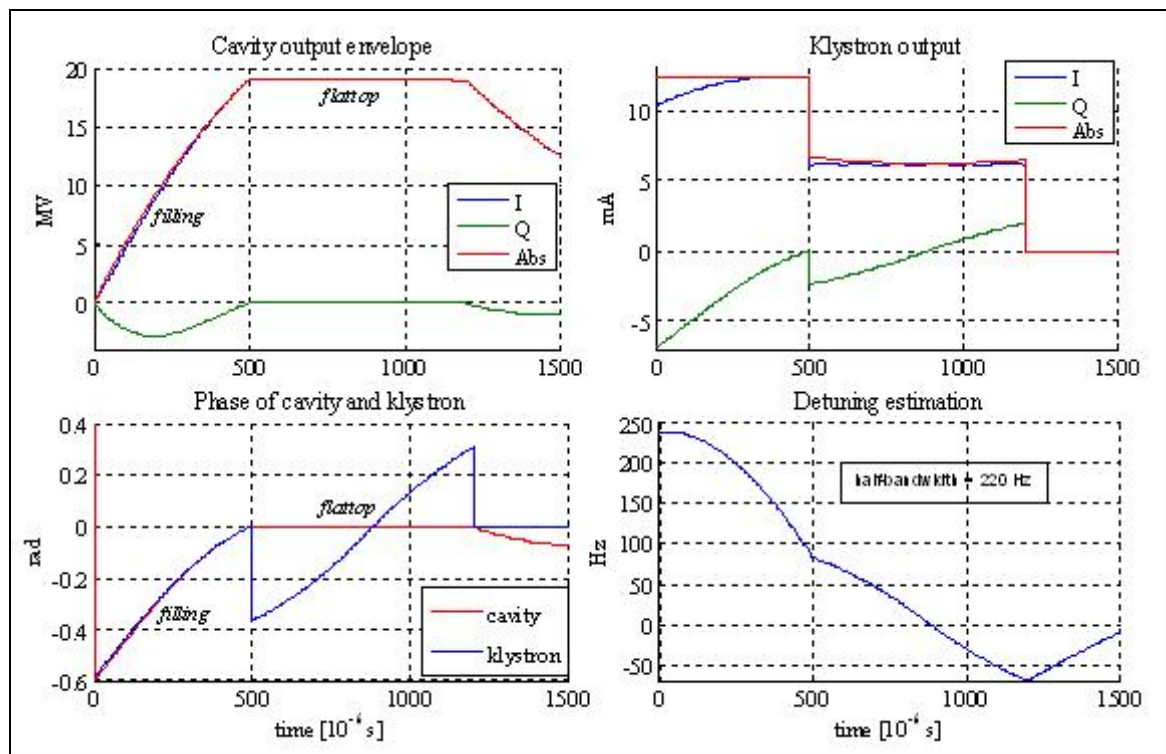


Figure 9.4 Feed Forward remote control for vector sum of MTS cavities (gain=0)

9.2 LLRF cost and reliability

9.2.2 Radiation damage study

During 2007 the radiation monitoring system RADMON (**R**adiation **M**onitor) installed in FLASH tunnel was extended (up to six permanently mounted sensors and two mobile) and tested. The radiation level is recorded on-line and stored for further processing.

We also performed experiments with various electronic components being irradiated in LINAC2 (linear electron accelerator at DESY site) tunnel, not only digital ones but analogue as well. The integrated circuits (reference voltage sources) were placed for the long time in the tunnel (3 months) and after irradiation the voltage was measured and compared to the initial one. Also the new IRES boards (IRradiation Experiments System) able to perform various tests of digital electronics e.g. SRAM (Static Random Memory) and FLASH memories and Virtex 5 FPGA chip) in radiation environment are under development (boards are designed and ready to produce).

The further development of software based fault detection and correction was also performed. The SIFT (Software Implemented Fault Tolerance) methods were being developed and implemented in a C++ compiler. They are based on automatically generated redundancy in software (redundant data and program flows) that allows detection and correction of radiation induced errors. The worked out methods, algorithms and software tools will be used in LLRF control system.

9.3 Hardware

9.3.1 Multichannel downconverter

During 2007 a new carrier board were designed and manufactured as shown in Figure 9.5. The digital motherboard can carry mezzanine (mezzanine board - an extension a motherboard) boards. Different VME (VERSA Module Eurocard bus) sized mezzanine boards for various applications are designed, namely

- Analog frontend multi-channel downconverters with integrated ADCs (),
- Analog high resolution ADCs for new beam arrival monitors,
- Analog high resolution ADCs for new beam position monitors.



Figure 9.5 Digital motherboard suited to carry mezzanine boards with downconverters and ADC

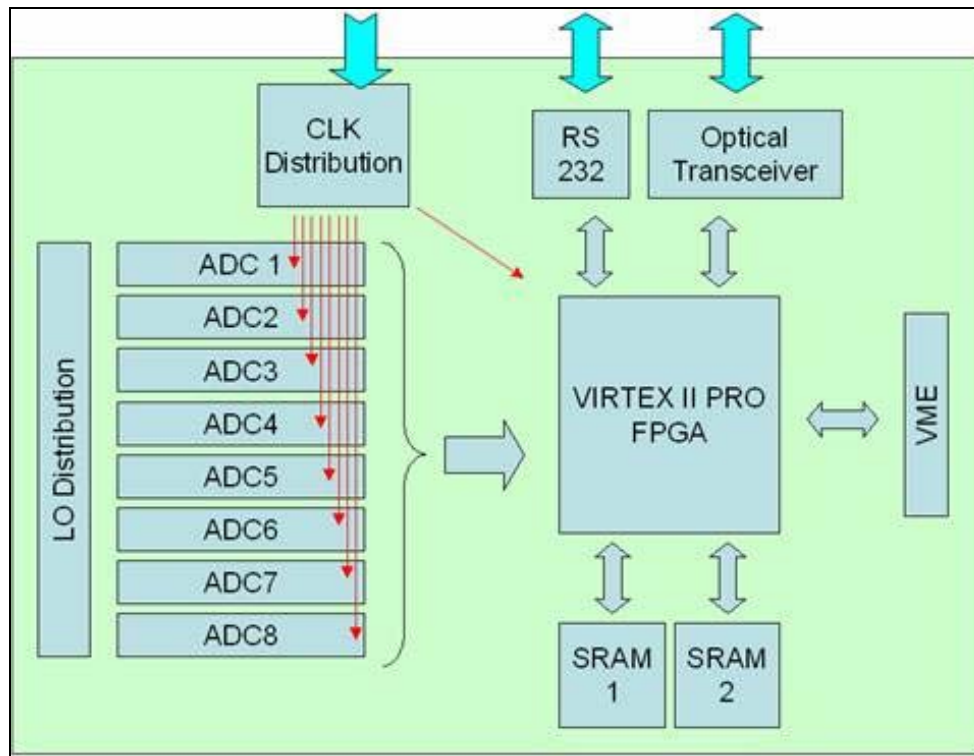


Figure 9.6 Block diagram of the digital VME carrier board.

As depicted in Figure 9.6, the carrier board provides a clock distribution, fast optical transceiver, VME interface, RAM and an FPGA for data pre-processing.

9.3.2 Third generation RF control

During 2007 the SIMCON DSP (SIMCON board equipped with DSP processor) board was tested and debugged. After making necessary corrections to the schematics 10 SIMCON DSP boards were manufactured (Figure 9.7). They will be used in the development of the control algorithms for LLRF.



Figure 9.7 Debugged control board SIMCON DSP

9.3.3 Stable frequency distribution

During the reporting period a new frequency distribution system was partially assembled and tested. The stability requirements of Master Oscillator (MO) were 100fs and 1ps for times shorter than 100ms and longer 1000s respectively. The frequency distribution system (Figure 9.8) consists of MO supplying several reference frequencies and power amplifiers for signals distribution. The low level part of the system is already finished. The implementation and testing of the power part of the system is in progress (Figure 9.9).

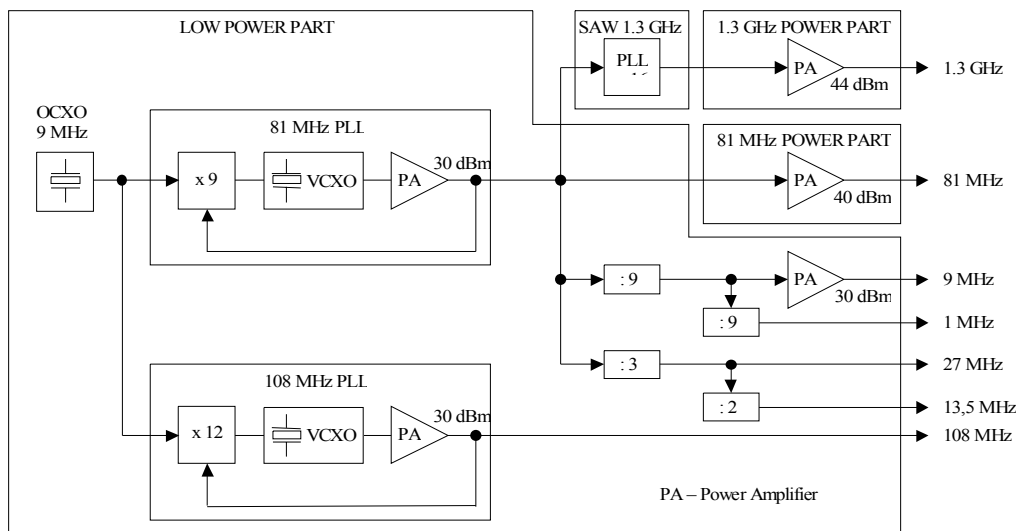


Figure 9.8 Block diagram of frequency distribution system



Figure 9.9 Frequency generation and distribution boxes

The RF infrastructures transfer from "l'Orme des Merisiers" to the main Saclay Center is now finished since May 2007, one year after the last RF test performed in CryHoLab.

Tests on cavity are only restarted at low RF power in vertical cryostat and not yet in the horizontal one CryHoLab (DI water is still not in operation at this time). Water supplying for cooling klystron, compressor and pumps is only planned for September; so high power RF, helium liquefying, and pumping on helium bath (test at 2 K) can not be possible before October.

Nevertheless preparation of the third series of tests in Cryholab related to the Saclay cold tuning system equipped with magnetostrictive element is on the way (figure 10.1):

- the mechanical part to adapt the magnetostrictive actuator on the cold tuning system is finished (figure 10.2 left),
- the whole system is already assembled on a 9-cell cavity (figure 10.2 right).

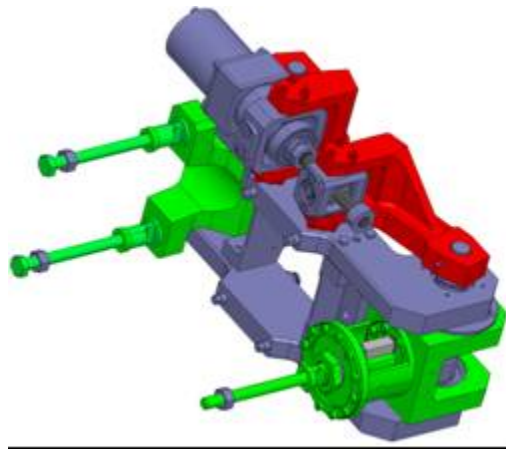


Fig.10.1 Cold Tuning System equipped with Magnetostrictive Actuator

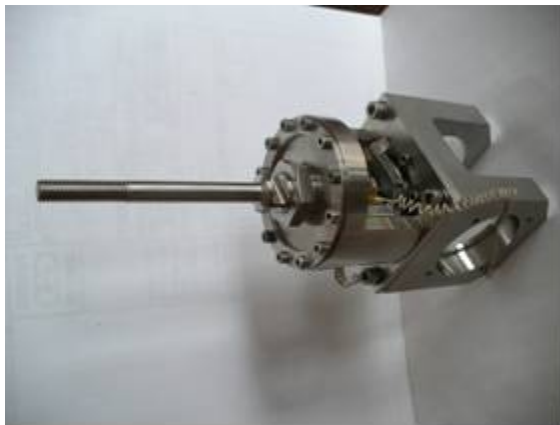
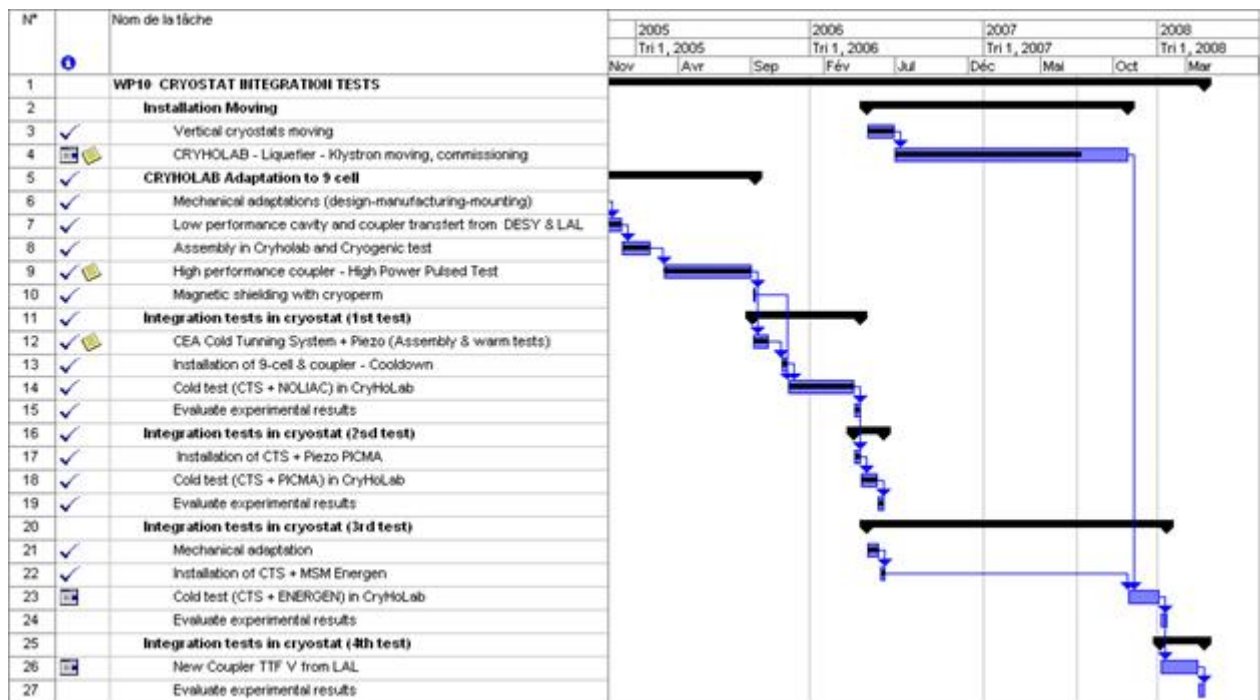


Fig.10.2 Magnetostrictive Actuator: mechanical part (left) – installation on a 9-cell cavity (right)



WP 11 Beam Diagnostics (BD)**Task 11.1: Beam position monitor**

Our objective was to improve the mechanical design and validate the copper coating in order to install the cavity BPM in a XFEL cryomodule. A second electronics is making to improve the resolution ($< 1 \mu\text{m}$) but reduce the dynamics range to $\pm 1 \text{ mm}$.

Mechanical design

To be installed in an X-FEL cryomodule, the alignment of the two parts composing the re-entrant BPM has to be improved. The copper plating has to be validated, too.

A cavity body (Fig. 11.1) was fabricated to adjust the alignment of two pieces and to validate the copper plating of the beam pipe. With a three-dimensional measurement, the alignment of two pieces was measured with an angle around 0.02° .



Figure 11.1: Two pieces of the re-entrant BPM

The copper plating was fabricated with the DESY specifications and its thickness was measured to be around $12.7 \mu\text{m}$. This copper plating was validated by DESY after a firing at 400°C for 2 hours and a complete cleaning procedure inclusive supersonic bath.

A cryogenic test was carried out at Saclay on twenty antennas (Fig 11.2).



Figure 11.2: Antenna of the re-entrant BPM

Each antenna was cooled, 3 times, in N_2 cold vapour then a leak test is carried out. Eighteen antennas passed this test.

The next cavity BPM in final design will be installed in a cold cryostat but won't be tested with beam.

Measurements

During the next studies at the end of August, the resolution will be improved in adding an amplifier on each channel, in the signal processing electronics. The Figure 11.3 shows the signal processing electronics with the amplifiers.

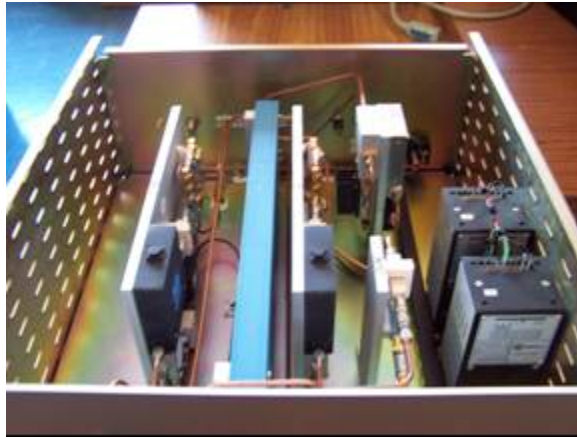


Figure 11.3: Signal processing electronics

As the limitation of the resolution is due to the ADCs noise, to improve the resolution, the dynamic range has to be reduced. With a dynamic range around ± 1 mm, the simulated resolution was calculated to be around $0.5 \mu\text{m}$.

WP 11.2 – Emittance monitor

In January 2006 a block of machine shifts were dedicated to the experiment of measuring the transverse beam dimension through the analysis of the Optical Diffraction Radiation (ODR) angular distribution.

The maximum beam energy achievable was of the order of 700 MeV, and the transport of the beam along the by-pass more comfortable. In these conditions, we succeeded in producing, at the ODR screen position, a beam narrower than the .5 mm slit, as it is shown in Fig. 11.4.

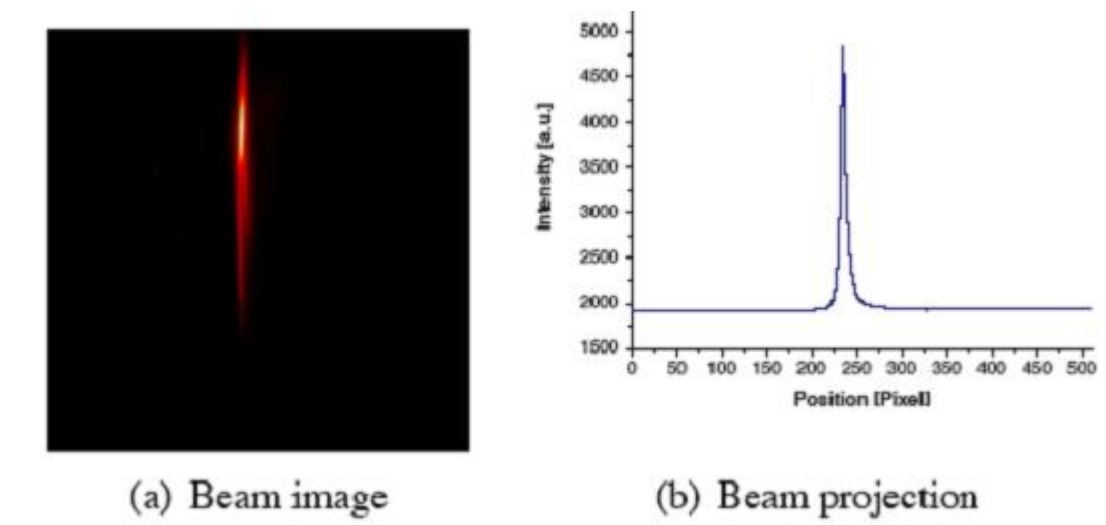


Figure 11.4: Image of the beam on the OTR screen (a) and its projection (b).

With the limitations due to a non complete background subtraction, moving the beam across the slit showed the expected behavior, and also the intensity dependence on the beam position was what expected from theory (see Fig. 11.5 and Fig. 11.6).

The minimum of the total intensity of Fig. 3 is obtained when the beam is perfectly centered inside the slit. In this position we performed a more accurate measurement, resulting in the profile shown in Fig. 11.7, together with a simulation obtained with the measured beam parameters.

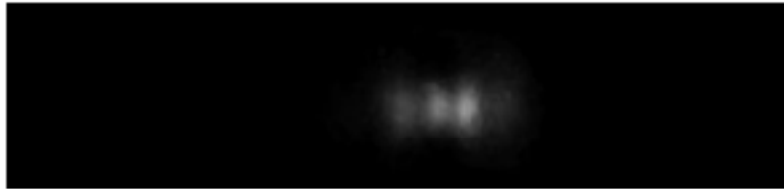
In this case we have also a good quantitative agreement with the experimental data, but the uncertainty that still remain about the effectiveness of the background subtraction prevents us to affirm that the real beam dimension can be extracted by the experimental data. To obtain this result, which is the final goal of the experiment, we need to reduce the impact of the background. This can be obtained in two different ways: increasing the beam energy will increase the signal level without affecting the noise, and the synchrotron radiation background itself can be largely stopped by a metallic screen with a slightly larger slit few centimeters in front of the detector screen.

A better lead shielding of the camera could also reduce the X rays background.

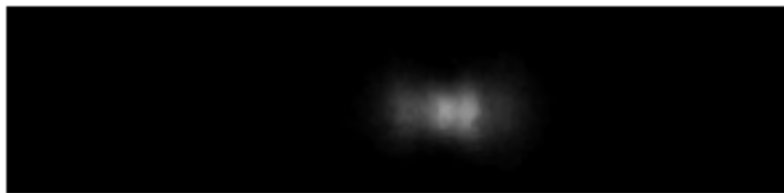
All these effects will be tested next year in the next machine study period.



(a) 0 μm



(b) 100 μm



(c) 200 μm

Figure 11.5: Vertically polarized angular distribution for different position of the beam within the slit.

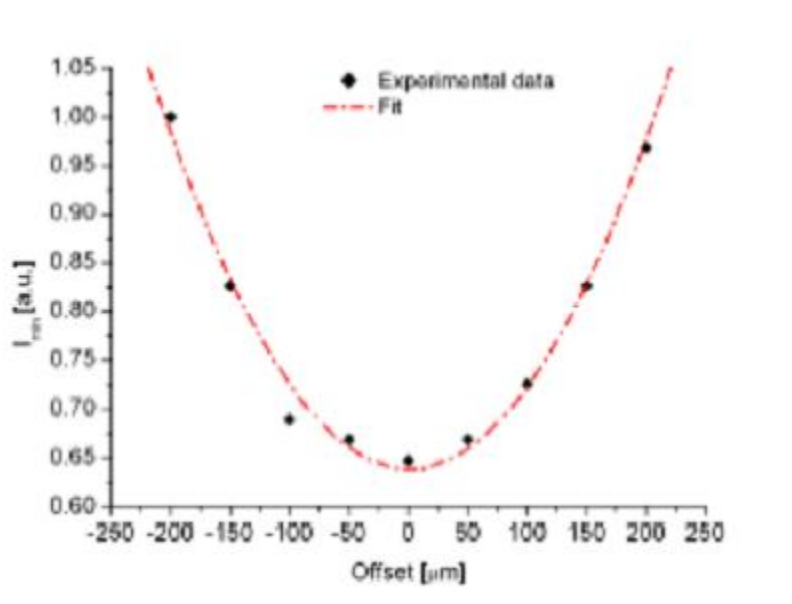


Figure 11.6: Measured dependencies of ODR minimum intensity as function of the displacement of the beam within the slit.

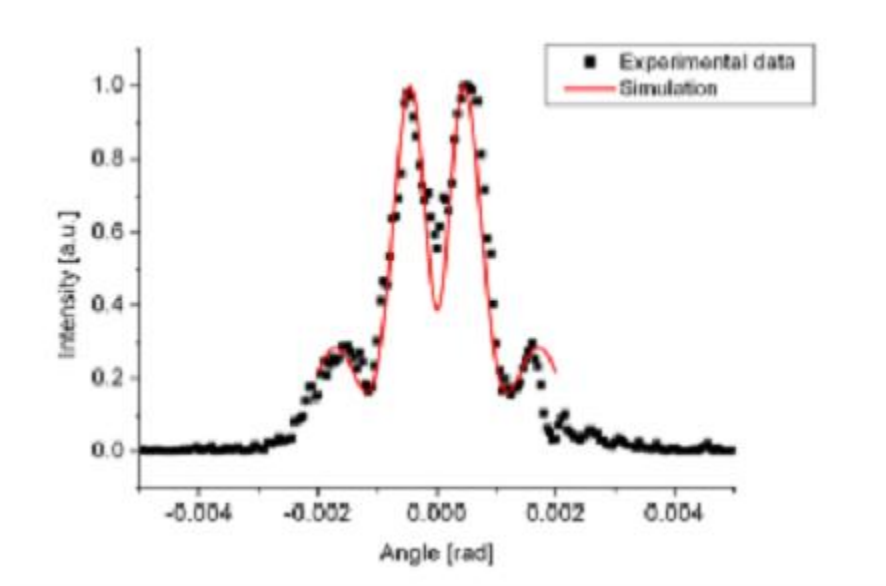


Figure 11.7: ODR angular distribution: 25 bunches, 0.7 nC per bunch, 0.5 mm slit. Polarizer and 800 nm filter are inserted.